LETTER

doi:10.1038/nature11811

Sustainable bioenergy production from marginal lands in the US Midwest

Ilya Gelfand[1,2], Ritvik Sahajpal[1,3,4], Xuesong Zhang[1,3], R. César Izaurralde[1,3,4], Katherine L. Gross[1,2,5] & G. Philip Robertson[1,2,6]

Legislation on biofuels production in the USA[1] and Europe[2,3] is directing food crops towards the production of grain-based ethanol[2,3], which can have detrimental consequences for soil carbon sequestration[4], nitrous oxide emissions[5], nitrate pollution[6], biodiversity[7] and human health[8]. An alternative is to grow lignocellulosic (cellulosic) crops on 'marginal' lands[9]. Cellulosic feedstocks can have positive environmental outcomes[10,11] and could make up a substantial proportion of future energy portfolios[12,13]. However, the availability of marginal lands for cellulosic feedstock production, and the resulting greenhouse gas (GHG) emissions, remains uncertain. Here we evaluate the potential for marginal lands in ten Midwestern US states to produce sizeable amounts of biomass and concurrently mitigate GHG emissions. In a comparative assessment of six alternative cropping systems over 20 years, we found that successional herbaceous vegetation, once well established, has a direct GHG emissions mitigation capacity that rivals that of purpose-grown crops (-851 ± 46 grams of CO_2 equivalent emissions per square metre per year ($gCO_2e\ m^{-2}\ yr^{-1}$)). If fertilized, these communities have the capacity to produce about 63 ± 5 gigajoules of ethanol energy per hectare per year. By contrast, an adjacent, no-till corn–soybean–wheat rotation produces on average 41 ± 1 gigajoules of biofuel energy per hectare per year and has a net direct mitigation capacity of $-397 \pm 32\ gCO_2e\ m^{-2}\ yr^{-1}$; a continuous corn rotation would probably produce about 62 ± 7 gigajoules of biofuel energy per hectare per year, with 13% less mitigation. We also perform quantitative modelling of successional vegetation on marginal lands in the region at a resolution of 0.4 hectares, constrained by the requirement that each modelled location be within 80 kilometres of a potential biorefinery. Our results suggest that such vegetation could produce about 21 gigalitres of ethanol per year from around 11 million hectares, or approximately 25 per cent of the 2022 target for cellulosic biofuel mandated by the US Energy Independence and Security Act of 2007, with no initial carbon debt nor the indirect land-use costs associated with food-based biofuels. Other regional-scale aspects of biofuel sustainability[2], such as water quality[11,14] and biodiversity[15], await future study.

US legislation mandates the annual production of 80 Gl of ethanol from non-grain sources by 2022[1], which will represent ~25% of projected best-case liquid transportation fuel needs by 2050. Although much of the land need could be satisfied by growing high-productivity feedstocks on fertile land now used for grain production[16], this strategy fails to consider the long-term need for fertile land to meet future food demands and the need to abate the indirect GHG impacts created when land now in grain ethanol production was originally diverted to biofuel use[4,17,18].

An alternative is to grow cellulosic crops on marginal lands[9]. Marginal lands are those poorly suited to field crops because of low crop productivity due to inherent edaphic or climatic limitations or because they are located in areas that are vulnerable to erosion or other environmental risks when cultivated. Often such lands are suitable for grasses, short-rotation tree crops or other perennial vegetation with persistent roots that are better adapted to low-nutrient, erodible or droughty soils. As long as the conversion of these lands to biofuel production avoids local carbon debt[4,19] and the replacement crop removes from the atmosphere more CO_2 than the pre-existing vegetation would have stored[17,19], cellulosic crops on marginal lands might provide substantial GHG emissions mitigation without the risk of indirect carbon costs due to displaced food and feed production[17]. Recent estimates place the indirect carbon costs for corn grain ethanol at 25–200 $gCO_2e\ MJ^{-1}$ (ref. 18), putting at risk much of the fossil fuel offset benefit of biofuels grown on arable land.

Still uncertain, however, are the availability of non-arable marginal lands for cellulosic feedstock production and the resulting implications for GHG emissions. First, not all marginal lands are sufficiently close to a potential biorefinery to make transportation economical. Second, the productivity of marginal lands can vary because of low-fertility soils and location-specific interactions between soils and climate. Third, not all cellulosic feedstocks deliver equivalent climate benefits: soil carbon sequestration, N_2O fluxes and other sources of global warming can differ widely among different feedstocks[20]. Of available cellulosic feedstocks, only existing herbaceous vegetation—or purpose-grown feedstocks such as switchgrass seeded into existing vegetation—avoids local carbon debt associated with land conversion and planting[4,9,17,19], but the potential productivity of this vegetation has been questioned[12] and there have been no long-term comparative analyses of its potential GHG benefits.

Here we provide a 20-yr comparative assessment of direct GHG benefits, or GHG balances, for six alternative biofuel cropping systems, including native successional vegetation, replicated at the Kellogg Biological Station (KBS) Long-term Ecological Research (LTER) site in southwest Michigan, USA. We compare GHG emissions and the productivity of established successional vegetation with those of both annual and perennial crops at a single, moderate-fertility location, without consideration of indirect carbon costs. We then project the potential for early successional vegetation to produce biofuel on marginal lands across a ten-state region of the US Midwest using a well-established quantitative crop productivity model calibrated at KBS for successional vegetation and tested elsewhere (Methods Summary). Our intent is to provide a conservative and realistic estimate of the capacity of marginal lands in the US Midwest to produce cellulosic biofuel without carbon debt[19] and without the added carbon cost of indirect land-use change[17].

Twenty-year patterns of GHG balances for the annual cropping systems (Table 1) show that without fossil fuel offsets, the conventionally managed system had a net release of GHG equivalents, whereas the no-till system accumulated enough soil carbon to offset the GHG costs of farming inputs and N_2O losses. In contrast to earlier results[20], the poplar system was also a net source of GHG, owing mainly to soil

[1]Great Lakes Bioenergy Research Center, Michigan State University, East Lansing, Michigan 48824, USA. [2]W.K. Kellogg Biological Station, Michigan State University, Hickory Corners, Michigan 49060, USA. [3]Joint Global Change Research Institute, Pacific Northwest National Laboratory and University of Maryland, College Park, Maryland 20740, USA. [4]Department of Geographical Sciences, University of Maryland, College Park, Maryland 20740, USA. [5]Department of Plant Biology, Michigan State University, East Lansing, Michigan 48824, USA. [6]Department of Plant, Soil, and Microbial Sciences, Michigan State University, East Lansing, Michigan 48824, USA.

Table 1 | Average annual GHG emissions for each candidate feedstock cropping system

Cropping system	Soil carbon*	N_2O†	CH_4†	Farming inputs‡							Net GHG balance
				N	P	K	Lime	Fuel	Seeds	Pest control	
Conventional CSW	0 ± 31	34 ± 6	−0.8 ± 0.1	32.7	0.4	1	3	13	7	7	98 ± 31
No-till CSW	−122 ± 31	35 ± 4	−0.8 ± 0.1	32.7	0.3	1	4	9	7	16	−20 ± 31
Alfalfa	−122 ± 92	33 ± 3	−1.0 ± 0.1	0	0.3	4	14	11	6	3	−52 ± 92
Poplar	61 ± 153	17 ± 3	−0.8 ± 0.0	3.3	0	0	0	1	0	2	84 ± 153
Successional	−397 ± 31	11 ± 1	−1.1 ± 0.1	0	0	0	0	0	0	0	−383 ± 31
Successional + N	−397 ± 31	27 ± 5	−1.2 ± 0.5	55.5	0	0	0	8	0	0	−308 ± 31

Values shown are means ± s.e. (n = 4–6; $gCO_2e\ m^{-2}\ yr^{-1}$), calculated without consideration of fossil fuel offset credits (Table 2) or the cost of indirect land use change for the period 1989–2009. For detailed information, see Supplementary Tables 1 and 6–10. CSW, corn–soybean–wheat rotation.
* A/A_p horizon (surface soil to plow depth), from ref. 21; there were no significant soil carbon changes in lower horizons to 1 m. For calculation see Supplementary Information, equation (2).
† n = 4.
‡ Rotational average.

carbon loss following harvest[21]. This is probably due to microbial activity stimulated by warmer and wetter soil conditions caused by the absence of shade and by lower transpiration by resprouting trees before canopy closure[22]. Conversely, alfalfa provided significant mitigation despite high N_2O fluxes. In the successional system, high rates of soil carbon accumulation and low N_2O emissions provided substantial mitigation under both unfertilized and fertilized conditions (Table 1).

Including fossil fuel offset credits makes all six systems net direct sinks of atmospheric CO_2. Biorefinery yields of 0.43 l of bioethanol per kilogram of dry corn grain and 0.38 l of cellulosic ethanol per kilogram of biomass[19,23,24] provide offsets of 280 ± 16 and 309 ± 10 $gCO_2e\ m^{-2}\ yr^{-1}$ for conventional and no-till annual crops; 319 ± 35 and 514 ± 14 $gCO_2e\ m^{-2}\ yr^{-1}$ for the perennial poplar and alfalfa; and 463 ± 34 and 624 ± 46 $gCO_2e\ m^{-2}\ yr^{-1}$ for unfertilized and fertilized successional systems (Fig. 1a and Table 2). Including these offsets in the GHG balance (Fig. 1b) results in net direct mitigation that ranges from −247 ± 35 to −397 ± 32 $gCO_2e\ m^{-2}\ yr^{-1}$ for the annual crops, from −241 ± 157 to −605 ± 93 $gCO_2e\ m^{-2}\ yr^{-1}$ for the perennial crops and from −851 ± 46 to −932 ± 55 $gCO_2e\ m^{-2}\ yr^{-1}$ for the successional communities (Table 2).

In absolute terms, energy production was highest for the fertilized successional system (63 ± 5 $GJ\ ha^{-1}\ yr^{-1}$) and lowest for poplar (30 ± 3 $GJ\ ha^{-1}\ yr^{-1}$); other systems had intermediate values of energy production (Table 2). Had the annual no-till crop rotation been continuous corn with county-average yields rather than being corn–soybean–wheat at KBS, we estimate that the energy yield would have been ~60% higher (62 ± 7 $GJ\ ha^{-1}\ yr^{-1}$) with a direct GHG balance ~13% less negative (Table 2). Although the GHG emission intensity of the fertilized successional system was higher than that of an unfertilized system (−147 ± 14 versus −197 ± 18 $gCO_2e\ MJ^{-1}$ for a 90% harvest efficiency), it remains substantially lower than that of most other systems examined, with a direct GHG emission reduction of 105% relative to fossil fuels (Table 2). In contrast, the wheat and corn portions of the annual rotations had GHG emission reductions of only 23 and 28%, respectively, although the equivalent soybean reduction was 240% owing to the allocation of emissions to co-products (Table 2).

The low mitigation potential of the poplar system is due to its relatively low productivity in addition to the soil carbon loss noted above. Additional fertilization[25] and protection from a 2-yr defoliation by

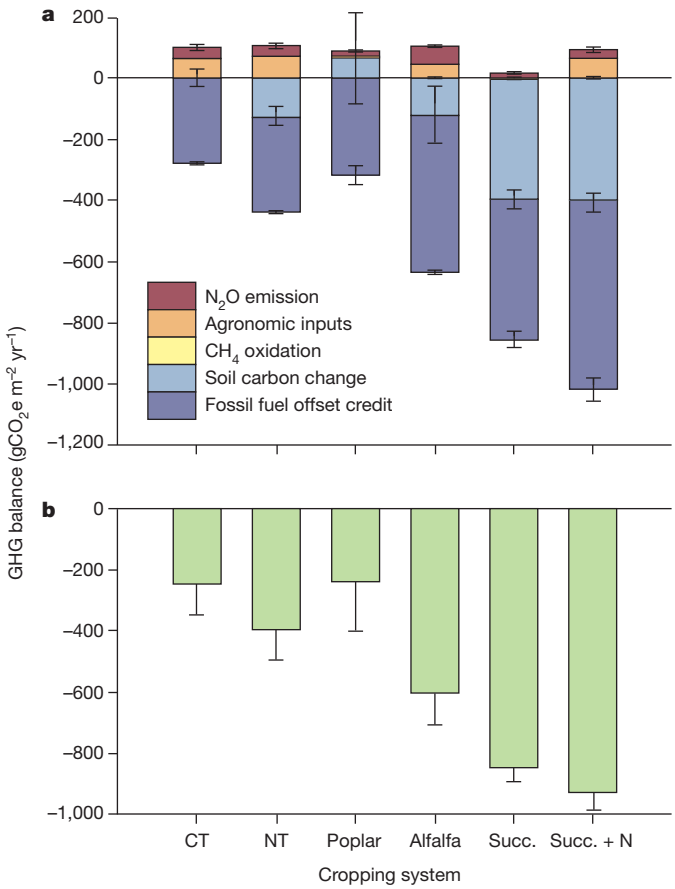

Figure 1 | GHG balances of alternative cropping systems in southwest Michigan for biofuel feedstock production. **a**, Detailed GHG balance; **b**, net GHG balance. Bars represent different components of the GHG balance for a given system and were measured as soil emissions of N_2O and CH_4 (1989–2010), changes in soil carbon (1989–2001), and agronomic inputs and yields (used to calculate fossil fuel credits) from 1989 to 2009. Agricultural inputs include GHG emissions from farm machinery, agricultural chemicals and crop seed production. Fluxes of CH_4 are insignificant and are too small to be visible in the figure. Errors, s.e. (n = 4–6 replicates). CT, conventionally tilled system; NT, no-till system.

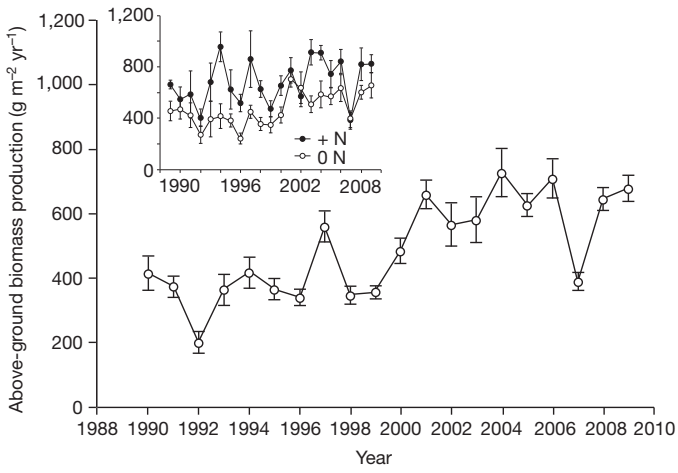

Figure 2 | Above-ground biomass production of the successional system between 1989 and 2009 in 1-ha treatment plots. Inset, effects of nitrogen fertilizer (+N; 124 $kgN\ ha^{-1}\ yr^{-1}$) and no fertilizer (0 N) in subplots. Errors, s.e. (n = 6).

Table 2 | Energy production, GHG emission intensity, GHG emission reduction, fossil fuel offset credit and net GHG balance for the cropping systems in Table 1

Cropping system	GHG emission intensity ($gCO_2e\ MJ^{-1}$)	Energy production ($GJ\ ha^{-1}\ yr^{-1}$)	GHG emissions reduction (%)	Fossil fuel offset credit ($gCO_2e\ m^{-2}\ yr^{-1}$)	Net GHG balance ($gCO_2e\ m^{-2}\ yr^{-1}$)
Conventional CSW*	−65 ± 11	38 ± 4	28 (C), 240 (S), 23 (W)	280 ± 16	−247 ± 35
No-till CSW	−97 ± 9	41 ± 2	31 (C), 240 (S), 25 (W)	309 ± 10	−397 ± 32
No-till CC†	−56 ± 12	62 ± 7	40 (C), 40 (C)	256 ± 52	−344 ± 60
Alfalfa	−119 ± 19	51 ± 1	111	514 ± 14	−605 ± 93
Poplar	−80 ± 52	30 ± 3	112	319 ± 35	−241 ± 157
Successional‡	−260 ± 24 to −197 ± 18	24 ± 2 to 43 ± 3	114	463 ± 34	−851 ± 46
Successional + N‡	−208 ± 19 to −147 ± 14	35 ± 3 to 63 ± 5	105	624 ± 46	−932 ± 55

Values shown are means ± s.e. ($n = 6$), except for GHG emissions reductions, which are given as per cent relative to gasoline ($94\ gCO_2\ MJ^{-1}$) for each grain crop in rotation (C, corn; S, soybean; W, wheat), the numbers are for grain based biofuels. For wheat straw, the GHG emissions reduction is 107%. Energy production was calculated from biomass yields (Supplementary Table 1). No corn or soybean stover was harvested for bioenergy production, owing to site-specific limitations to protect soil carbon, whereas wheat straw was harvested.

* Use of average corn yields for Kalamazoo county instead of KBS (Supplementary Methods) would increase fossil fuel offset credit for the rotation by 8% ($303 \pm 10\ gCO_2e\ m^{-2}\ yr^{-1}$) and the overall net GHG balance by 9% ($-270 \pm 33\ gCO_2e\ m^{-2}\ yr^{-1}$).

† Estimated values for a no-till corn–corn (CC) rotation with all grain and 17% of stover removed for bioethanol production, including a 10% continuous-corn-rotation yield penalty (Supplementary Table 1). Fossil fuel offset credits are from ref. 19; for calculation of the GHG emissions reduction, we used relative contributions of corn grain and corn stover ethanol to total GHG reduction. For net GHG balance, we assumed that soil emissions of N_2O and CH_4 and soil carbon sequestration rates were similar to measured rates in the no-till CSW rotation.

‡ The range for the successional system reflects a 55% contemporary and 90% potential harvest efficiency.

gypsy moths[26] might have improved poplar yield in its first rotation. On average, nitrogen fertilization boosted yields by 47% in the successional system (Fig. 2, inset, and Supplementary Table 1) and provided a fossil fuel offset credit greater by 35% (Table 2). Although the carbon cost of additional fertilizer and the N_2O flux it induced (Table 1) negate part of the net GHG gain in the fertilized successional system (Fig. 1), the higher productivity with fertilization allows for greater land-use intensity from these systems with little additional carbon cost.

We used the Environmental Policy Integrated Climate (EPIC) model[27–29] to estimate the productivity of fertilized and unfertilized successional systems (Table 1 and Fig. 1) across a ten-state region of the US Midwest. The model was run on a fine-grained spatial scale (0.4-ha resolution) to capture interactions between local soils and climates and to allow modelled cells within an explicit geographic area to be aggregated by distance. Simulated annual yields for unfertilized marginal lands in the region averaged $6 \pm 3\ Mg\ ha^{-1}\ yr^{-1}$ (Supplementary Table 2). Simulated fertilization at $68\ kgN\ ha^{-1}\ yr^{-1}$ (kgN, kilograms of nitrogen) increased average yields by 36% to $8 \pm 3\ Mg\ ha^{-1}\ yr^{-1}$ (Supplementary Table 2), which is consistent with measured fertilization response over grasslands in North America[30] and with measured estimates of on-farm switchgrass production within the region[31]. Our modelled estimates of switchgrass productivity correlate well with those of successional vegetation (Pearson correlation coefficient, $R^2 = 0.94$; Supplementary Fig. 1).

For the region, total modelled yield sums to $262\ Tg\ yr^{-1}$ (Supplementary Table 3). Of this, about 58%, or $152\ Tg\ yr^{-1}$, are produced within 80 km of 35 potential biorefineries, each with a minimum feedstock requirement of $653 \times 10^3\ Mg\ yr^{-1}$ (Supplementary Information, equation (1)). This provides a total fossil fuel offset of up to $44\ TgCO_2e\ yr^{-1}$ (Fig. 3, Supplementary Fig. 2 and Supplementary Table 3). Total ethanol production for all biorefineries sums to $20.8\ Gl\ yr^{-1}$ and represents ~27% of the cellulosic ethanol mandated by the US Energy Independence and Security Act of 2007[1]. The 80-km collection radius is optimal for the current distribution of marginal lands in the region. With no biorefinery minimum feedstock requirement, maximum production would decline by ~5% were the collection radius increased to 120 km ($19.2\ Gl\ yr^{1}$) or decreased to 40 km ($19.3\ Gl\ yr^{-1}$) (Supplementary Fig. 3). A fine-scale distributed network of smaller processing facilities[24] would relax the constraint imposed by the 80-km collection radius and increase collectable biomass from the 42% now excluded.

Not all lands classified as marginal for crop production are idle; on average about 8% of our biomass production areas are grazed (with a range of 0–71%), which reduces our estimate of available biomass from marginal lands by as much as 10% (Supplementary Table 3). Depending on collection radii and biorefinery size restrictions, excluding grazed areas from our analysis lowers our estimated biomass production to $136\ Tg\ yr^{-1}$, for a fossil fuel offset of $39\ TgCO_2e\ yr^{-1}$ and an ethanol yield of $18.6\ Gl\ yr^{-1}$ (Supplementary Table 4).

In contrast to earlier estimates of potential cellulosic feedstock availability in ref. 12, our analysis limits production to marginal lands and uses a process-based crop model operating on a fine-grained scale to estimate biomass yields, rather than estimating yields by statistical extrapolation to both marginal and cropped land. A state-by-state yield comparison reveals little relationship between the average yields predicted by the two approaches ($R^2 = 0.008$; Supplementary Table 5). Overall, our approach predicts average yields that are 20% lower than those projected by ref. 12.

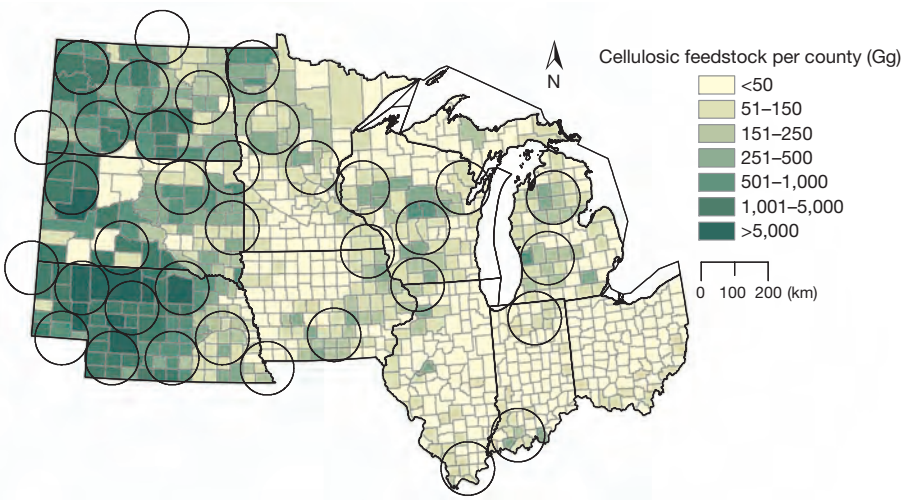

Figure 3 | Potential biomass collection areas for cellulosic biorefineries within ten US midwest states. Each circle represents an area of 80-km radius with sufficient biomass resources to produce at least 89 Ml of cellulosic ethanol per year, according to quantitative simulation of yields from fertilized successional vegetation on non-forested marginal lands at a resolution of 60 m × 60 m. County-scale totals of marginal lands biomass production are shown in green.

Restoring or improving the productivity of marginal lands while using them as biofuel cropping systems might allow them to contribute even more to US energy and GHG mitigation goals in addition to providing greater conservation benefits. Many marginal lands are degraded and not managed, others simply have low productivity, and still others are environmentally sensitive and perhaps in set-aside programs such as the US Department of Agriculture's Conservation Reserve Program. Our results show that management allowing the continued growth of perennial herbaceous species on these lands, undisturbed but for harvest and fertilization, could avoid the carbon costs of conversion, forgone sequestration and indirect land-use change. Furthermore, management could promote the establishment and growth of highly productive species such as future switchgrass cultivars with high nitrogen-use efficiency. This would provide additional GHG benefits in the form of increased energy yields, nitrogen fertilizer savings and greater soil carbon sequestration[17], and might concomitantly improve site fertility[32]. Other aspects of biofuel sustainability[2] not considered here, such as landscape-scale water quality[11,14] and biodiversity benefits[15], might be readily co-managed.

METHODS SUMMARY

GHG emissions quantification. We studied six ecosystems established in southwest Michigan[20] in 1989 at the KBS LTER site (http://lter.kbs.msu.edu). We compared two 3-yr rotations of corn (*Zea mays* L.), soybean (*Glycine max* (L.) Merrill) and wheat (*Triticum aestivum* L.) with all grain biomass and wheat straw used for biofuel production (Supplementary Table 1). One system was chisel-plowed (conventional tillage) and the other was permanent no-till. We also analysed three perennial systems: alfalfa (*Medicago sativa* L.), short-rotation poplar trees (*Populus* × *canadensis Moench* var. *eugenei*) and a successional old-field system that has been burned biannually since 1997 and annually since 2002. In the successional system, we compared biomass production with and without nitrogen fertilization. For each system, we constructed total net GHG (CO_2e) budgets that include the carbon costs of all farming operations and inputs from 1989 to 2009 (Supplementary Tables 6–8) and measured fluxes of N_2O and CH_4 for the period 1991–2010 (Supplementary Table 9), the annual accumulation of soil carbon to 1 m for the period 1989–2001 (Supplementary Table 10) and fossil fuel offset credits calculated from the biomass produced weighted by ethanol and biodiesel life cycle impacts (Supplementary Table 11). None of our GHG budgets include estimates of indirect GHG impact associated with diverting food crops to biofuel production[17,18]. The total net GHG budget for an equivalent no-till, continuous corn rotation was calculated using average corn yields of Kalamazoo County, Michigan and fossil fuel offset credits from ref. 19, together with the net GHG balance of the no-till system.
Regional productivity modelling. The EPIC model was evaluated for successional vegetation growing on former agricultural fields with above-ground net primary production data from the KBS and Cedar Creek, Minnesota LTER sites (Supplementary Materials). Yields for biofuel feedstock production were then simulated across a ten-state region at a resolution of 60 m × 60 m (Supplementary Table 3).

Full Methods and any associated references are available in the online version of the paper.

Received 29 March; accepted 20 November 2012.
Published online 16 January 2013.

1. US 110th Congress. *Energy Independence and Security Act of 2007*. Public Law 110–140; http://www.gpo.gov/fdsys/pkg/PLAW-110publ140/pdf/PLAW-110publ140.pdf (2007).
2. Robertson, G. P. *et al.* Sustainable biofuels redux. *Science* **322,** 49–50 (2008).
3. Fischer, G. *et al.* Biofuel production potentials in Europe: sustainable use of cultivated land and pastures, part II. Land use scenarios. *Biomass Bioenergy* **34,** 173–187 (2010).
4. Fargione, J., Hill, J., Tilman, D., Polasky, S. & Hawthorne, P. Land clearing and the biofuel carbon debt. *Science* **319,** 1235–1238 (2008).
5. Crutzen, P. J., Mosier, A. R., Smith, K. A. & Winiwarter, W. N_2O release from agro-biofuel production negates global warming reduction by replacing fossil fuels. *Atmos. Chem. Phys.* **8,** 389–395 (2008).
6. Donner, S. D. & Kucharik, C. J. Corn-based ethanol production compromises goal of reducing nitrogen export by the Mississippi River. *Proc. Natl Acad. Sci. USA* **105,** 4513–4518 (2008).
7. Landis, D. A., Gardiner, M. M., van der Werf, W. & Swinton, S. M. Increasing corn for biofuel production reduces biocontrol services in agricultural landscapes. *Proc. Natl Acad. Sci. USA* **105,** 20552–20557 (2008).
8. Hill, J. Polasky, S. Nelson, E., Tilman, D. & Huo, H. Climate change and health costs of air emissions from biofuels and gasoline. *Proc. Natl Acad. Sci. USA* **106,** 2077–2082 (2009).
9. Tilman, D., Hill, J. & Lehman, C. Carbon-negative biofuels from low-input high-diversity grassland biomass. *Science* **314,** 1598–1600 (2006).
10. Meehan, T. D., Hurlbert, A. H. & Gratton, C. Bird communities in future bioenergy landscapes of the upper midwest. *Proc. Natl Acad. Sci. USA* **107,** 18533–18538 (2010).
11. Robertson, G. P., Hamilton, S. K., Del Grosso, S. J. & Parton, W. J. The biogeochemistry of bioenergy landscapes: carbon, nitrogen, and water considerations. *Ecol. Appl.* **21,** 1055–1067 (2011).
12. Perlack, R. D. *et al. US Billion-Ton Update: Biomass Supply for a Bioenergy and Bioproducts Industry*. Report No. ORNL/TM-2011/224 (US DOE, 2011).
13. Ohlrogge, J. *et al.* Driving on biomass. *Science* **324,** 1019–1020 (2009).
14. Dominguez-Faus, R., Powers, S. E., Burken, J. G. & Alvarez, P. J. The water footprint of biofuels: a drink or drive issue? *Environ. Sci. Technol.* **43,** 3005–3010 (2009).
15. Webster, C. R., Flaspohler, D. J., Jackson, R. D., Meehan, T. D. & Gratton, C. Diversity, productivity and landscape-level effects in North American grasslands managed for biomass production. *Biofuels* **1,** 451–461 (2010).
16. Somerville, C., Youngs, H., Taylor, C., Davis, S. C. & Long, S. P. Feedstocks for lignocellulosic biofuels. *Science* **329,** 790–792 (2010).
17. Searchinger, T. D. *et al.* Fixing a critical climate accounting error. *Science* **326,** 527–528 (2009).
18. Plevin, R. J. & Kammen, D. M. in *Encyclopedia of Biodiversity* (ed. Levin, S. A.) (Elsevier, in the press).
19. Gelfand, I. *et al.* Carbon debt of Conservation Reserve Program (CRP) grasslands converted to bioenergy production. *Proc. Natl Acad. Sci. USA* **108,** 13864–13869 (2011).
20. Robertson, G. P., Paul, E. A. & Harwood, R. R. Greenhouse gases in intensive agriculture: contributions of individual gases to the radiative forcing of the atmosphere. *Science* **289,** 1922–1925 (2000).
21. Syswerda, S. P., Corbin, A. T., Mokma, D. L., Kravchenko, A. N. & Robertson, G. P. Agricultural management and soil carbon storage in surface vs. deep layers. *Soil Sci. Soc. Am. J.* **75,** 92–101 (2011).
22. Stoffel, J. L., Gower, S. T., Forrester, J. A. & Mladenoff, D. J. Effects of winter selective tree harvest on soil microclimate and surface CO_2 flux of a northern hardwood forest. *For. Ecol. Manage.* **259,** 257–265 (2010).
23. Kim, S. & Dale, B. E. Life cycle assessment of various cropping systems utilized for producing biofuels: bioethanol and biodiesel. *Biomass Bioenergy* **29,** 426–439 (2005).
24. Eranki, P. L. & Dale, B. E. Comparative life cycle assessment of centralized and distributed biomass processing systems combined with mixed feedstock landscapes. *GCB Bioenergy* **3,** 427–438 (2011).
25. Coleman, M. *et al.* Post-establishment fertilization of Minnesota hybrid poplar plantations. *Biomass Bioenergy* **30,** 740–749 (2006).
26. Kosola, K., Dickmann, D., Paul, E. & Parry, D. Repeated insect defoliation effects on growth, nitrogen acquisition, carbohydrates, and root demography of poplars. *Oecologia* **129,** 65–74 (2001).
27. Izaurralde, R. C., Williams, J. R., McGill, W. B., Rosenberg, N. J. & Jakas, M. C. Q. Simulating soil C dynamics with EPIC: model description and testing against long-term data. *Ecol. Modell.* **192,** 362–384 (2006).
28. Zhang, X. *et al.* An integrative modeling framework to evaluate the productivity and sustainability of biofuel crop production systems. *GCB Bioenergy* **2,** 258–277 (2010).
29. Soil Survey Staff. Soil Survey Geographic Database. *National Resources Conservation Service* http://soildatamart.nrcs.usda.gov (USDA, 2011).
30. Clark, C. M. *et al.* Environmental and plant community determinants of species loss following nitrogen enrichment. *Ecol. Lett.* **10,** 596–607 (2007).
31. Schmer, M. R., Vogel, K. P., Mitchell, R. B. & Perrin, R. K. Net energy of cellulosic ethanol from switchgrass. *Proc. Natl Acad. Sci. USA* **105,** 464–469 (2008).
32. Fornara, D. A. & Tilman, D. Ecological mechanisms associated with the positive diversity productivity relationship in an N-limited grassland. *Ecology* **90,** 408–418 (2009).

Supplementary Information is available in the online version of the paper.

Acknowledgements We thank S. Bohm, K. A. Kahmark, I. Shcherbak, and S. VanderWulp for help with data assembly; C. McMinn, J. Simmons and many others for field and laboratory assistance; J. R. Williams for EPIC model advice; and D. H. Manowitz for programming and computational assistance. We are additionally indebted to B. Bond-Lamberty, B. E. Dale, V. H. Dale, J. D. Hill, W. M. Post and T. O. West for comments on an earlier version of the manuscript. Financial support for this work was provided by the US DOE Office of Science (DE-FC02-07ER64494, KP1601050) and Office of Energy Efficiency and Renewable Energy (DE-AC05-76RL01830, OBP 20469-19145), the US National Science Foundation LTER program (DEB 1027253), NASA (NNH08ZDA001N), and MSU AgBioResearch. EPIC simulations were performed on the PNNL Evergreen computer cluster, which is supported by the US DOE Office of Science (DE-AC05-76RL01830).

Author Contributions G.P.R., I.G. and R.C.I. designed the study. I.G., R.C.I., R.S. and X.Z. analysed data and wrote initial drafts of the manuscript. R.C.I., R.S. and X.Z. performed simulations. X.Z. designed the spatially explicit modelling system. K.L.G. designed and performed the fertilization study. I.G. and G.P.R. wrote the final version of the manuscript.

Author Information Reprints and permissions information is available at www.nature.com/reprints. The authors declare no competing financial interests. Readers are welcome to comment on the online version of the paper. Correspondence and requests for materials should be addressed to I.G. (igelfand@msu.edu) or G.P.R. (robert30@ msu.edu).

METHODS

GHG sampling and calculation of CO_2 equivalents. The CO_2 equivalents ($gCO_2e\,m^{-2}\,yr^{-1}$) for N_2O and CH_4 emissions were calculated using IPCC 100-yr horizon factors[33] (Supplementary Information, equations (3) and (4)). Measurements of soil GHG fluxes (Supplementary Table 9) were performed bi-weekly using a static-chamber method[20]. Cumulative emissions of N_2O (grams per hectare of nitrogen from N_2O) and CH_4 (grams per hectare of carbon from CH_4) for each plot were determined by interpolating daily fluxes between sampling days over the course of the entire growing season from first thaw in late winter until soils froze in late autumn during 1989–2010.

Farming CO_2e calculation. Total GHG emissions associated with farming (Supplementary Tables 6–8) were calculated as the sum of CO_2e emissions from the production of fertilizers and herbicides and from farm agricultural machinery fuel use. Calculations (Supplementary Information, equation (5)) were based on actual field practice at the study sites, with average fuel use and production costs from published tables[20,34–37] and the LTER Narrative Agronomic Field Log (http://lter.kbs.msu.edu/datatables/16). For perennial and successional systems, GHG emissions were calculated on a yearly basis.

Calculation of fossil fuel displacement due to the use of renewable fuels. We used results of published analyses for the calculation of fossil fuel displacement due to the use of renewable fuels and their co-products, or fossil fuel offset credits, similar to the procedure explained in ref. 19.

For carbon offsets due to biodiesel production, we used published results for the GREET life cycle analysis model[38], which compares five different approaches for crediting GHG emissions allocations to co-products: a displacement approach, an allocation approach based on the energy value of co-products, an allocation approach based on the market value of co-products and two hybrid approaches that integrate the displacement and allocation methods. We used the approach based on the energy value of co-products, which sums to 7.6 $kgCO_2e$ per kilogram of soybean diesel, or 193.9 $gCO_2e\,MJ^{-1}$ using a biodiesel energy yield of 34.5 $MJ\,l^{-1}$ and a diesel volumetric density of 0.88 $g\,ml^{-1}$ (refs 39, 40). Of this sum, 1.16 $kgCO_2e$ per kilogram of biodiesel is allocated to soy meal, 1.29 $kgCO_2e\,kg^{-1}$ to glycerin, 1.08 $kgCO_2e\,kg^{-1}$ to fuel gas (displacing natural gas), 0.76 $kgCO_2e\,kg^{-1}$ to heavy oil, 0.20 $kgCO_2e\,kg^{-1}$ to propane fuel mix, 0.96 $kgCO_2e\,kg^{-1}$ to product gas, 0.99 $kgCO_2e\,kg^{-1}$ to light cycle gas and 1.15 $kgCO_2e\,kg^{-1}$ to clarified slurry oil[38].

Further, we substituted our measured emissions from agricultural inputs for the 39.4 $gCO_2e\,MJ^{-1}$ estimated by the GREET model, which are based on emissions of 278 $gCO_2e\,kg^{-1}$ for produced soybean grain (GREET, version 1.8d.1). More specifically, GREET assumes farm energy use of 825.9 kJ per kilogram of soybean grain produced (21,310 BTU per bushel); additionally, GREET assumes the following farming inputs (per kilogram of soybean grain): 1.9 g N fertilizer, 5.6 g P_2O_5, 11.2 g K_2O, 157.0 g $CaCO_3$, 0.5 g herbicides and 0.001 g insecticide. One kilogram of soybean grain can produce 0.205 l of biodiesel (using conversion factors as above), which will contain 7.1 MJ of energy. For conversion of GREET assumptions to an areal basis, we assume an average production of 2.5 $Mg\,ha^{-1}$ (average soybean grain yield in Kalamazoo county, Michigan[18]). Thus, using our site soybean yields and GREET assumptions, we calculate, for our site, emissions of 69.2 $gCO_2e\,m^{-2}$ during soybean farming (278 gCO_2e per kilogram of soybeans × 2,489 kg soybeans per hectare).

Using measured farming activities (Supplementary Tables 6–8), we calculate that overall emissions from farming during the average soybean rotational year in KBS LTER fields were lower than assumed in the GREET and summed to 10.2 and 11.1 $gCO_2e\,m^{-2}\,yr^{-1}$ for conventionally tilled and no-till systems, respectively (Supplementary Table 11). Using a similar procedure to calculate GHG emissions per energy unit ($gCO_2e\,MJ^{-1}$; see above), we estimate that KBS LTER emissions sum to 7.1 and 6.8 $gCO_2e\,MJ^{-1}$ of biodiesel energy for conventionally tilled and no-till systems, respectively. Thus, we added the difference between emissions from agricultural inputs in both cases (32.3 and 32.6 $gCO_2e\,MJ^{-1}$) to the carbon offset of biodiesel, calculated by the GREET model. This makes our fossil fuel offset value greater than those estimated by GREET, that is, 225.6 and 225.9 $gCO_2e\,MJ^{-1}$ of biodiesel energy produced for conventionally tilled and no-till systems, respectively (Supplementary Table 11). Average soybean yields for our sites were between 2.0 and 2.3 $Mg\,ha^{-1}\,yr^{-1}$ or ~217 $g\,m^{-2}\,yr^{-1}$ (Supplementary Table 1), which could produce ~39 g of biodiesel per square metre, or ~1.5 $MJ\,m^{-2}$, and thus could offset ~339 $gCO_2e\,m^{-2}\,yr^{-1}$.

For carbon offsets associated with the production of corn grain ethanol, we used a comparison between results of life cycle analysis by the EBAMM and GREET models, with the latter using dry milling for corn ethanol production[38,41,42]. We estimate the CO_2e cost of producing, distributing and combusting fossil gasoline at 94.0 gCO_2e per megajoule of gasoline energy, calculated from the EBAMM model as reported in ref. 41. For estimation of the CO_2e costs of production and distribution of corn ethanol, we used management data from our site for the agricultural phase and the corn ethanol scenario from GREET (version 1.8.d.1).

Using measured farming activities (Supplementary Tables 6 and 7), we calculate that overall emissions from farming during the average corn rotational year at KBS LTER fields are between 72.9 and 73.0 $gCO_2e\,m^{-2}\,yr^{-1}$ for conventionally tilled and no-till systems, respectively (Supplementary Table 8) or 37.7 and 34.7 $gCO_2e\,MJ^{-1}$, respectively, on the basis of KBS yields (Supplementary Table 1) and agricultural inputs used for the Fuel_Prod_TS module of the GREET model. In GREET, the emissions associated with the agricultural part of corn ethanol production sum to 36.1 $gCO_2e\,MJ^{-1}$ (GREET, version 1.8.d.1); the differences between GREET and measured emissions are associated with differences in agricultural inputs such as fertilizers and energy and assumed crop yield. For example, GREET assumes 15.3 gN fertilizer per kilogram of corn, whereas our measured values are 21.4 gN per kilogram of corn. Assumed P and K use, on the other hand, was larger in the GREET model than at KBS: 5.8 versus 6.8 gP per kilogram of corn and 0.3 versus 1.4 gK per kilogram of corn (GREET versus KBS). Agricultural lime usage also was higher in GREET than at KBS: 45.3 versus 1.3 g per kilogram of corn. Energy-use assumptions in GREET were similar to measured values: ~0.4 and ~0.5 MJ per kilogram of corn, respectively. Finally, the actual yields at KBS were lower than assumed in the GREET (9.9 versus 6.1 Mg of corn per hectare for GREET and KBS, respectively), owing to rainfall variability over the period examined; irrigated yields at KBS are ~13 Mg of corn per hectare (Supplementary Materials). We assumed no emissions associated with land-use change for our long-cropped, well-equilibrated KBS soils. All emissions associated with the ethanol production phase in GREET were accounted for without adjustments (except yield differences).

We used these estimates for calculations of overall emissions from corn grain ethanol production, and adjusted CO_2e offsets generated by the GREET model accordingly, similar to estimates of CO_2e emissions from the production of soybeans (above). We thus estimate that overall emissions from corn-based ethanol for KBS are 68.1 and 65.1 gCO_2e per megajoule of ethanol energy for conventionally tilled and no-till systems, respectively (37.7 and 34.7 $gCO_2e\,MJ^{-1}$ for the agricultural part and 30.4 $gCO_2e\,MJ^{-1}$ for the biorefinery part), after adjustment of assumed GREET inputs to measured KBS inputs. In comparison, overall emissions calculated by GREET (version 1.8.d.1) were 66.5 $gCO_2e\,MJ^{-1}$: 36.1 and 30.4 $gCO_2e\,MJ^{-1}$ for the agricultural and biorefinery parts of the cycle, respectively. This makes the estimated fossil fuel offset credits for KBS very similar to that estimated by GREET for average corn grain ethanol production across the United States. This analysis accounts for CO_2e emissions from farm operations, transportation and biorefinery operations. Thus, we estimate the net reduction in CO_2e emissions as the difference between emissions from the production, distribution and combustion of fossil gasoline (94.0 $gCO_2e\,MJ^{-1}$; EBAMM, release 1.1[42,43]) and the distribution and production of corn ethanol, for net savings of 25.9 and 28.9 gCO_2e per megajoule of corn ethanol energy produced by KBS fields under conventional and no-till management, respectively.

For ethanol produced from wheat grain, we adjusted GREET model inputs to those actually measured at KBS for wheat farming, and estimated overall emissions from the agricultural phase in GREET to be 37.8 and 35.6 gCO_2e per megajoule of ethanol energy for conventionally tilled and no-till systems, respectively. Although the GREET model has no wheat scenario, we assumed that the use of measured agricultural inputs and wheat yields provides a good approximation of the emissions associated with wheat production, especially because other farming activities (travel of workers to farm fields, labour input, machinery production and so on) are similar in wheat and corn farming. Furthermore, we assumed that the ethanol distillation phase of corn ethanol does not differ significantly from that of wheat ethanol.

We used GREET-generated CO_2e emissions per megajoule of energy to estimate potential fossil fuel offset credits when wheat grain is used for bioethanol production, that is, 25.8 and 28.0 $gCO_2e\,MJ^{-1}$ for conventionally tilled and no-till systems, respectively. Although we assumed that the biorefinery part of wheat ethanol production is similar to that of corn ethanol production, the energy value of wheat ethanol co-products, dried distillers grains with solubles, is on average 17% lower than that of corn dried distillers grains with solubles[43]. Thus, we reduced the fossil fuel offset calculated from GREET for wheat grain ethanol further by 17%, with offset final values of 21.4 and 23.2 $gCO_2e\,MJ^{-1}$ for conventionally tilled and no-till systems, respectively. For cellulosic ethanol from wheat straw, we estimated net CO_2e offsets of 108.3 gCO_2e per megajoule of ethanol energy for both types of management, after allocation of all agricultural emissions to wheat grain production.

For the estimation of fossil fuel offsets for scenarios with cellulosic ethanol production from poplar, alfalfa and herbaceous vegetation (successional and successional +N), we similarly used comparisons of emissions assumed in GREET with those measured at our site. Emissions associated with agricultural inputs assumed in GREET, 6.6 and 18.6 $gCO_2e\,MJ^{-1}$ for the production of tree and herbaceous vegetation, respectively, were different from those measured at

our sites: 2.3, 8.0, 1.0 and 9.9 $gCO_2e\,MJ^{-1}$ for poplar, alfalfa, successional and successional + N systems, respectively (Supplementary Table 8). Furthermore, we adjusted GREET-generated fossil fuel carbon offset values for measured emissions. We estimate that production of 1 MJ of energy from cellulosic feedstock in the alfalfa scenario would save 103.3 gCO_2e and that the savings would be 105.0 $gCO_2e\,MJ^{-1}$ in the poplar scenario and 107.3 and 98.4 $gCO_2e\,MJ^{-1}$ in the successional and successional + N scenarios, respectively (Supplementary Table 8). Under the original GREET assumptions, ethanol production would save 89.7 $gCO_2e\,MJ^{-1}$ from herbaceous vegetation and 100.7 $gCO_2e\,MJ^{-1}$ from the farmed woody biomass.

To calculate the potential energy produced from biofuels, we used average KBS LTER yields, harvestable biomass from the successional treatment (Supplementary Table 1) and ethanol energy content (lower heating value assumed to be 21.1 MJ per litre of ethanol). We assumed a biorefinery yield of 0.43 l of bioethanol per kilogram of dry corn and wheat grain; 0.38 l of bioethanol per kilogram of dry wheat straw, corn stover and cellulosic biomass[19,44]; and 0.21 l of biodiesel per kilogram of soybean grain[39,40]. The energy-equivalent amounts of fossil fuel use avoided due to the use of biofuels were calculated (Supplementary Information, equation (6)) using lower-heating-value energy contents (34.5 and 21.1 $MJ\,l^{-1}$ for biodiesel and ethanol, respectively) and the specific densities of each fuel[19,40,45].

To compare the sustainability of biofuel production between different scenarios, we estimated the GHG emission intensity ($gCO_2e\,MJ^{-1}$), defined here as the net CO_2e balance per unit of biofuel energy produced in the system (Supplementary Information, equations (7)–(8)).

Model simulations of plant biomass yields at regional scales. We used the EPIC model[46–48] to simulate plant biomass yields on regional scales (for site-specific simulations and sensitivity analysis, see Supplementary Methods and Supplementary Figs 4 and 5). EPIC is a comprehensive biophysical process model capable of simulating plant yield and net primary productivity for diverse types of vegetation using weather, terrain, soil and management data. To simulate plant growth, EPIC uses radiation-use efficiency[49] to calculate the potential daily photosynthetic biomass production. Calculated daily potential growth is decreased proportionately by the most severe stress due to non-optimal conditions of water, nutrients (N and P), air and soil temperatures, soil acidity and soil salinity. EPIC has undergone comprehensive validation for a wide range of soils, management practices and climates in the United States[50] and across the world[51].

Regional EPIC simulations. We implemented an EPIC-based, spatially explicit integrative modelling framework[48] to simulate yields of perennial species grown on marginal lands across the ten-state study area in the US north-central region (Supplementary Fig. 6). This region extends from North Dakota in the northwest corner to Nebraska in the southwest corner, Ohio in the southeast corner, and Michigan in the northeast corner. The Canadian–US border defines the northern border of the study region. A spatially explicit geospatial database containing soil, terrain, weather, land-use/land-cover and management data was used to obtain relevant parameters for running the EPIC model. Details of the geospatial database follow.

Soils. Soil Survey Geographic data from the US Department of Agriculture Geospatial Data Gateway (http://datagateway.nrcs.usda.gov) were used to create a conterminous-scale soil property database at ~30-m scale. Properties included the number of soil layers; layer depth; slope gradient and length; bulk density; pH; per cent sand, silt, clay and coarse fragments; and per cent organic carbon and total nitrogen. To define marginal lands, we also extracted the land capability class (LCC) variable, which describes land classes on the basis of use limitation such as erosion risk, soil depth, wetness and slope[52]. There are eight LCCs, ranging from class I (lands without any limitations for agricultural use) to class VIII (lands with severe limitations). Classes I–IV can support cropland agriculture, whereas classes V–VIII contain non-arable land.

Topography. To derive topographical information, we used data from NASA's Shuttle Radar Topography Mission, which produced a digital elevation model for the region at a resolution of 30 m (ref. 53). Geospatial analysis was used to derive slope length and gradient for each spatial modelling unit.

Climate data. EPIC requires daily weather information including daily temperature (maximum and minimum), precipitation, solar radiation, wind speed and relative humidity. The North America Regional Reanalysis database (http://www.esrl.noaa.gov/psd/data/gridded/data.narr.html) was used to derive daily weather files at 32-km resolution[54].

Land use and land cover. The US National Agricultural Statistical Service's cropland data layer for 2008[55] and the Soil Survey Geographic database (ref. 29, accessed 26 August 2011) were combined to define land use, land cover and soil type at a spatial resolution of 60 m for the simulation domain. We excluded vegetation that has been planted in recreational areas such as parks or golf courses, vegetation for erosion control in developed areas and vegetation on federal lands.

Marginal lands. Marginal lands were identified as rural lands falling into LCCs V–VII with slope gradients of <20% (Supplementary Table 12) under non-forested vegetation. Available data sets do not allow us to distinguish between marginal lands readily available for biofuel feedstocks production and areas currently grazed. We use the cropland data layer estimate for grazed land to provide a maximum worst-case estimate, recognizing that only a portion of this estimate will fall into LCCs V–VII with slope gradients of <20%.

We gave special consideration to the Sandhills region of Nebraska, where unique grass-stabilized sand dune topography distinguishes the dunes from the surrounding prairies[56]. The sand dunes can be 100 m tall and several kilometres long. To exclude the highly erodible dune ridges and slopes from the analysis, we used the topographic position index algorithm in ArcGIS[57]. This index is a classification scheme based on the difference in elevation value between a cell in a digital elevation model raster and its neighbours. The extent to which a cell is higher or lower than its neighbours, combined with its slope, can be used to assign it a landform classification such as valley, slope or ridge. Removing the dune ridges and slopes from the analysis reduced the area available for consideration as marginal lands by more than 200,000 ha. The interdune valleys falling into LCCs V–VII and with slope gradients of <20% were then used for further analysis.

EPIC simulations and identification of biorefinery locations. For each grid of marginal land, we simulated above-ground net primary productivity using the calibrated EPIC model with three levels of nitrogen fertilization: 0, 68 and 123 $kgN\,ha^{-1}\,yr^{-1}$. Modelled field size for the estimation of potential productivity varied substantially, with a minimum size of 0.36 ha and a maximum of $>650 \times 10^3$ ha. Overall, we simulated 78,184 fields having unique combinations of soil type, land use and LCC. The connectivity between each field and nearby fields was not assessed. The maximum potential overlap of our defined marginal lands with grazing lands within each potential biorefinery circle ranges from 0 to 71%, with a regional maximum average of ~8% (Supplementary Table 3).

The values of above-ground net primary productivity obtained from EPIC (Supplementary Tables 2 and 3) were used to identify the location of potential biorefineries that could process the cellulosic feedstocks to ethanol production (Supplementary Information, equation (1)). We limited potential biorefineries to areas where potential feedstock production in fertilized (68 $kgN\,ha^{-1}\,yr^{-1}$) simulations were at least 653 $Gg\,yr^{-1}$ of cellulosic biomass on marginal lands from within an economically feasible transportation distance of 80 km (ref. 58). For this, we used a moving-window algorithm over the ten-state US midwest region and aggregated biomass yields from marginal lands falling within an 80-km-radius circle. Subsequently, non-overlapping circles with the highest biomass yields were selected for potential biorefinery locations. Actual locations of circles are partly dependent on geographic starting points for the moving-window analysis.

33. Forster, P. *et al.* in *Climate Change 2007: The Physical Science Basis* (eds Solomon, S. *et al.*) 129–234 (Cambridge Univ. Press, 2007).
34. West, T. O. & Marland, G. A synthesis of carbon sequestration, carbon emissions, and net carbon flux in agriculture: comparing tillage practices in the United States. *Agric. Ecosyst. Environ.* **91,** 217–232 (2002).
35. Lal, R. Carbon emission from farm operations. *Environ. Int.* **30,** 981–990 (2004).
36. Stein, D. 2008-2009 Custom Machine and Work Rate Estimates. *MSUE District Farm Business Management* https://www.msu.edu/user/steind/ (2009).
37. Syswerda, S. P., Basso, B., Hamilton, S. K., Tausig, J. B. & Robertson, G. P. Long-term nitrate loss along an agricultural intensity gradient in the Upper Midwest USA. *Agric. Ecosyst. Environ.* **149,** 10–19 (2012).
38. Huo, H., Wang, M., Bloyd, C. & Putsche, V. Life-cycle assessment of energy use and greenhouse gas emissions of soybean-derived biodiesel and renewable fuels. *Environ. Sci. Technol.* **43,** 750–756 (2009).
39. Sheehan, J. *et al. Life Cycle Inventory of Biodiesel and Petroleum Diesel for Use in an Urban Bus.* Report No. NREL/SR-580-24089 (USDA, 1998).
40. Patzek, T. W. A first law thermodynamic analysis of biodiesel production from soybean. *Bull. Sci. Technol. Soc.* **29,** 194–204 (2009).
41. Farrell, A. E. *et al.* Ethanol can contribute to energy and environmental goals. *Science* **311,** 506–508 (2006).
42. Plevin, R. J. Modeling corn ethanol and climate: a critical comparison of the BESS and GREET models. *J. Ind. Ecol.* **13,** 495–507 (2009).
43. Nuez Ortín, W. G. & Yu, P. Nutrient variation and availability of wheat DDGS, corn DDGS and blend DDGS from bioethanol plants. *J. Sci. Food Agric.* **89,** 1754–1761 (2009).
44. Kim, S. & Dale, B. E. Life cycle assessment of various cropping systems utilized for producing biofuels: bioethanol and biodiesel. *Biomass Bioenergy* **29,** 426–439 (2005).
45. Oak Ridge National Laboratory. Bioenergy conversion factors. http://www.localenergy.org/pdfs/Document Library/Bioenergy conversion factorspdf (2011).
46. Williams, J. R. in *Computer Models of Watershed Hydrology* (ed. Singh, V. P.) 909–1000 (Water Research Publications, 1995).
47. Izaurralde, R. C. *et al.* Simulating soil C dynamics with EPIC: model description and testing against long-term data. *Ecol. Modell.* **192,** 362–384 (2006).

48. Zhang, X. *et al.* An integrative modeling framework to evaluate the productivity and sustainability of biofuel crop production systems. *GCB Bioenergy* **2,** 258–277 (2010).
49. Sinclair, T. R., Muchow, R. C. & Donald, L. S. Radiation use efficiency. *Adv. Agron.* **65,** 215–265 (1999).
50. Izaurralde, R. C., Rosenberg, N. J., Brown, R. A. & Thomson, A. M. Integrated assessment of Hadley Center (HadCM2) climate-change impacts on agricultural productivity and irrigation water supply in the conterminous United States: Part II. Regional agricultural production in 2030 and 2095. *Agric. For. Meteorol.* **117,** 97–122 (2003).
51. Tan, G. & Shibasaki, R. Global estimation of crop productivity and the impacts of global warming by GIS and EPIC integration. *Ecol. Modell.* **168,** 357–370 (2003).
52. Klingebiel, A. A. & Montgomery, P. H. *Land-Capability Classification* (USDA, 1961).
53. Farr, T. G. *et al.* The shuttle radar topography mission. *Rev. Geophys.* **45,** RG2004 (2007).
54. Mesinger, F. *et al.* North American regional reanalysis. *Bull. Am. Meteorol. Soc.* **87,** 343–360 (2006).
55. Johnson, D. M. & Mueller, R. The 2009 cropland data layer. *Photogramm. Eng. Remote Sensing* **76,** 1201–1205 (2010).
56. Eggemeyer, K. D. *et al.* Ecophysiology of two native invasive woody species and two dominant warm-season grasses in the semiarid grasslands of the Nebraska sandhills. *Int. J. Plant Sci.* **167,** 991–999 (2006).
57. Tagil, S. & Jenness, J. GIS-Based automated landform classification and topographic, landcover and geologic attributes of landforms around the Yazoren Polje, Turkey. *J. Appl. Sci.* **8,** 910–921 (2008).
58. Bailey, C., Dyer, J. F. & Teeter, L. Assessing the rural development potential of lignocellulosic biofuels in Alabama. *Biomass Bioenergy* **35,** 1408–1417 (2011).

doi:10.1038/nature11811

Supplementary Figures

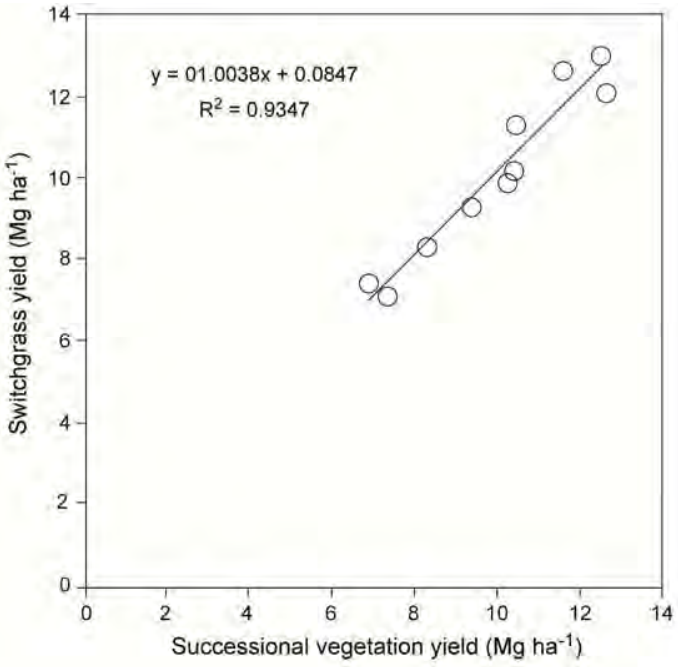

Supplementary Figure 1. Comparison of EPIC-simulated state-level average yields of post-establishment switchgrass (y-axis) and well-established successional vegetation (x-axis) in the US Midwest with nitrogen fertilization at 68 kg N ha^{-1} yr^{-1}. Results are from a sensitivity test of EPIC simulations to vegetation type. We examined the extent to which yields of grass mixes simulated across the 10-state US Midwest related to the simulated yields of N-fertilized switchgrass (*Panicum virgatum*), a model biomass crop also used in the Billion Ton Study[1]. Overall, there was a strong correlation between modeled yields, with R^2 = 0.935, and the Spearman rank-order correlation coefficient (r_s) = 0.952 with a two-tailed p-value of 0.000023. An r_s value above 0 implies positive agreement between the two rankings, suggesting that the KBS successional community can serve as a proxy of other perennial herbaceous systems including switchgrass. In general, we observe that modeled switchgrass yields at the state level in the Dakotas and Nebraska compare favorably with reported on-farm yields observed on marginal lands[2].

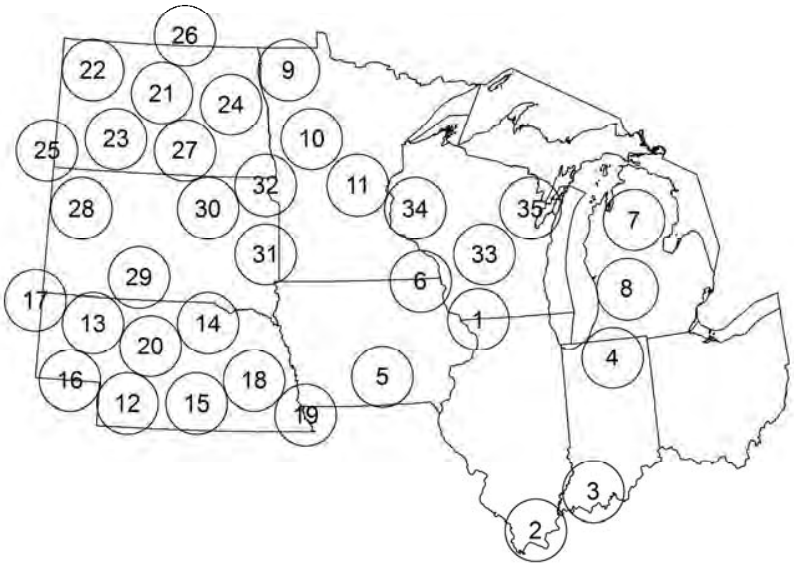

Supplementary Figure 2. The placement of biorefineries for cellulosic biomass production from marginal lands in ten US Midwest states with identification numbers corresponding to entries in Supplementary Table 3. Each circle represents an 80 km radius area with sufficient biomass resources to produce at least 89 ML ethanol yr^{-1} based on quantitative simulation of yields from non-forested marginal lands at a 60×60 m resolution.

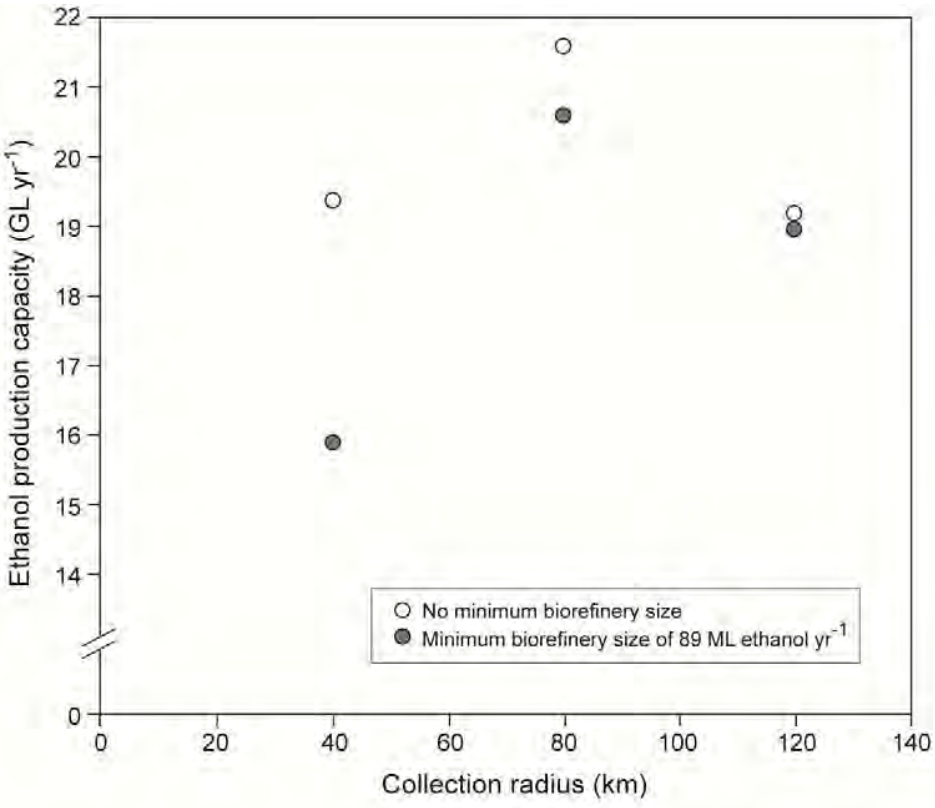

Supplementary Figure 3. Estimates of regional ethanol production as affected by the size of the biomass collection area (collection radius). Open circles denote production with no constraint on minimum biorefinery size; closed circles constrain collection areas to those with enough biomass to support a biorefinery producing at least 89 ML ethanol yr^{-1}. Note discontinuous y-axis.

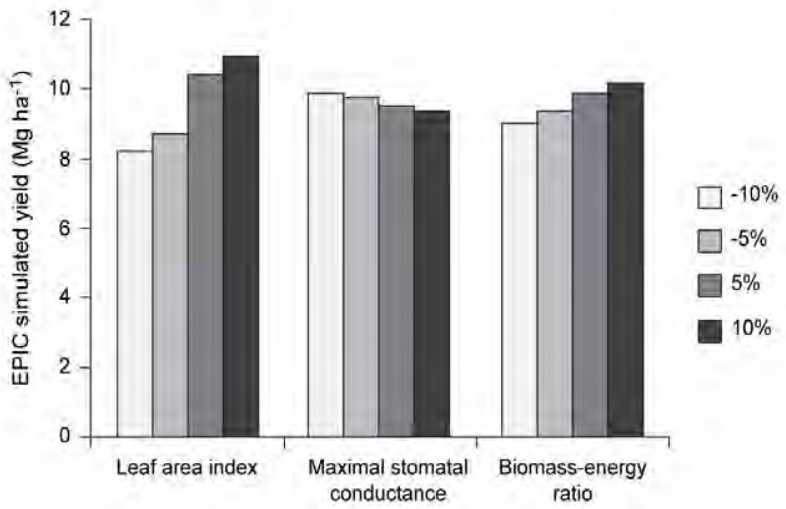

Supplementary Figure 4. Sensitivity of EPIC modeled results at KBS to three key model parameters: leaf area index (LAI), maximal stomatal conductance, and biomass-energy ratio. These model parameters were varied by ±5% and ±10%. Results are from a sensitivity test of EPIC simulations to crop parameters. The EPIC model has been shown to be sensitive to a variety of crop and soil parameters[3,4]. Based on these studies, we selected three crop parameters (biomass-energy ratio, LAI, and stomatal conductance) to perform sensitivity tests of EPIC under KBS conditions by varying these parameters from -10% to +10% in 5% increments. EPIC yields showed the greatest sensitivity to changes in LAI and similar levels of sensitivity to changes in biomass-energy ratio and stomatal conductance.

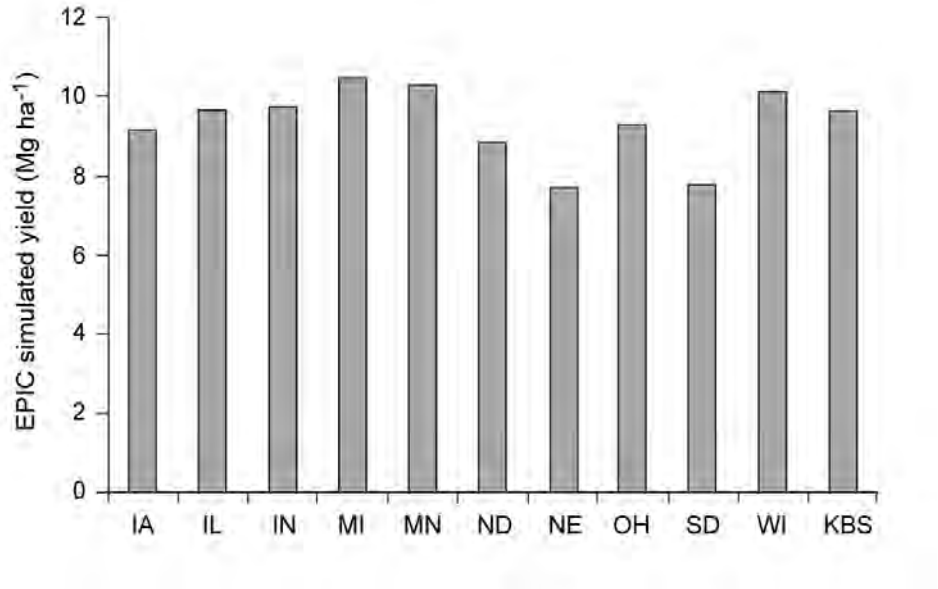

Supplementary Figure 5. Sensitivity of EPIC modeled results at KBS to climatic variations and soil drivers. The North America Regional Reanalysis (NARR) climate record closest to the centroid of each state was used to run the EPIC model for KBS. EPIC simulations were performed with KBS management and soil properties under 10 representative climates, one from each state. EPIC yields were sensitive to climatic drivers as suggested by a 2.8 Mg ha^{-1} yield range. To examine model sensitivity to soil properties, we ran EPIC with KBS weather and management and all the soils present in the surrounding KBS area. Average yield was 10.4±0.9 Mg ha^{-1} (n=10). Variation in total soil profile organic carbon was the most important factor contributing to yield; it explained 71% of the total variation simulated (y = 275.0x - 2644).

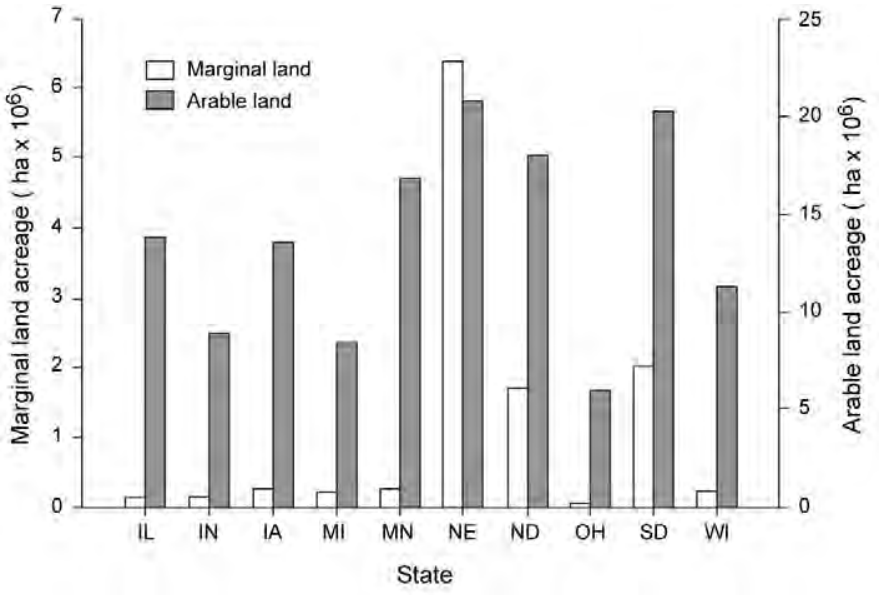

Supplementary Figure 6. Marginal lands acreage ($\times 10^6$ ha) in 10 states of the US Midwest, as modeled by EPIC (left Y axis, note the difference in scale between left and right Y axis; open bars) and arable land acreage (right Y axis; shaded bars) from Cropland Data Layer of 2008. States names given by standard abbreviation; IL – Illinois, IN – Indiana, IA – Iowa, MI – Michigan, MN – Minnesota, NE – Nebraska, ND – North Dakota, OH – Ohio, SD – South Dakota, WI – Wisconsin.

Supplementary Tables

Supplementary Table 1. Average yields of studied ecosystems (mean ± s.e., n = 6); C=corn, S= soybean, W=wheat. [†]

System	Corn yield	Wheat yield	Soybean yield	Cellulosic biomass [*]
	Mg ha^{-1} yr^{-1} dry mass			
Conventional tillage C-S-W	4.9 (0.4)	3.1 (0.1)	2.0 (0.1)	4.8 (0.1)
No-till C-S-W	5.4 (0.1)	3.3 (0.1)	2.3 (0.0)	4.8 (0.1)
No-till C-C	5.9 (0.6)			1.0 (0.6)
Alfalfa [‡]	-	0.2 (0.0)	-	6.4 (0.2)
Poplar	-	-		3.8 (0.4)
Successional [¶]	-	-	-	3.3 (0.2) – 5.4 (0.4)
Successional + N [¶]	-	-	-	4.8 (0.4) – 7.9 (0.6)

[†] Grain yield dry mass is calculated from yields reported at standard moisture (soybean and wheat at 13% moisture, corn at 15.5% moisture). Stover and straw biomass calculations for annual crops are based on standard harvest indices (HI = grain / [grain + stover]); HI for Conventional tillage corn and wheat are 0.51 and 0.39, respectively, and for No-till 0.52 and 0.41, respectively. For C offset calculations, the relative contribution of rotational crop yields were used: over 20 years of KBS LTER management corn has been planted 40% of the time, soybean 35%, and wheat 25%. For potential bioenergy production we used all produced grain (corn, soybean, wheat) and straw (wheat). We did not use corn stover production in order to maintain soil organic matter, which in SW Michigan requires stover inputs of 5.2 Mg ha^{-1} yr^{-1} for continuous corn and 7.8 Mg ha^{-1} yr^{-1} for corn–soybean rotations[5,6]; these management practices have maintained soil carbon concentrations over last 20 years (see Supplementary Table 10, and [7]). For the No-till continuous corn rotation scenario we used average corn yields of 7.7±0.8 Mg ha^{-1} yr^{-1} from Kalamazoo County, MI (2007 – 2009, average), less a 10% yield reduction penalty typical for continuous vs. rotational corn[8].

[*] Cellulosic biomass includes wheat straw.

[‡] Includes wheat grain and straw production during the grain break year prior to periodic re-establishment of the alfalfa stand due to weed encroachment and self-toxicity. The average yield for grain break years (3.2 ± 0.1 Mg dry mass ha^{-1} yr^{-1}) was calculated as the average wheat yield of conventional tillage and No-till systems, with one grain break year during the studied period. For alfalfa yields estimation we used machine harvest yields from the KBS LTER site for years 1995, 2002 – 2004, and 2006.

[¶] For estimation of harvestable cellulosic biomass we used average ANPP from Successional treatments of the KBS LTER site between years 2000 and 2009, after initial stabilization of biomass produced by these plots between 1989 and 2000 (dataset: http://lter.kbs.msu.edu/datatables/40; Fig. 1). From the dataset used for estimation of Successional ANPP we removed a small "standing dead" biomass pool due to our inability to attribute "standing dead" to biomass produced during a given season. The ANPP for this period averaged 598±44 g dry matter m^{-2} yr^{-1}. For the Successional + N treatment we estimate an ANPP of 879±64 g dry matter m^{-2} yr^{-1} based on the yield ratio between the

fertilized and unfertilized sub-plots (average ANPP for 1989-2009, n = 6; Fig 1 inset). Successional harvestable biomass reflects a 55% contemporary and 90% potential harvest efficiency[9,10,11].

Supplementary Table 2. Average biomass and ethanol yields for 78,184 parcels of marginal land as modeled by EPIC for three levels of N fertilizer application and two harvest efficiencies. Values in parentheses are standard deviations. Ethanol yields are based on a conversion factor of 380 L Mg^{-1} of cellulosic biomass (Supplementary Eq. 1).

Factor	Average Yields	
	Biomass	Ethanol
	Mg ha^{-1} yr^{-1}	*L×10^{3} ha^{-1} yr^{-1}*
Harvest efficiency (*%*)		
55	4.3 (1.7)	1.6 (0.6)
90	6.0 (2.6)	2.3 (1.0)
N Fertilization (*kg ha^{-1} yr^{-1}*) †		
0	6.0 (2.6)	2.3 (1.0)
68	8.2 (2.7)	3.1 (1.0)
123	8.9 (2.8)	3.3 (1.0)

† Simulations under different N fertilization regimes with assumed 90% harvest efficiency.

Supplementary Table 3. EPIC modeled biomass and cellulosic ethanol production by potential refineries within a given state assuming 90% harvest efficiency and two N-fertilization levels (0 and 68 kg N ha^{-1}). Refineries are numbered in states with more than one refinery.

ID[§]	*State*	Total biomass production per biorefinery area		Total cellulosic ethanol production		Total fossil fuel offset		Grazed land[††]	Total biomass production without grazed land		Total fossil fuel offset without grazed land	
		Mg × 10^6		*GL yr^{-1}*		*Mg CO_2e×10^6*		*%*	*Mg × 10^6*		*Mg CO_2e×10^6*	
		F*=0	F=68	F=0	F=68	F=0	F=68		F=0	F=68	F*=0	F=68
1	Illinois 1[‡]	1.35	1.88	0.18	0.26	0.38	0.46	62.3	0.51	0.71	0.16	0.20
2	Illinois 2	0.67	0.80	0.09	0.11	0.20	0.23	46.3	0.36	0.43	0.11	0.12
3	Indiana 1[‡]	1.18	1.43	0.16	0.19	0.29	0.33	52.7	0.56	0.68	0.17	0.19
4	Indiana 2[‡]	0.77	0.96	0.11	0.13	0.25	0.27	31.1	0.53	0.66	0.16	0.19
5	Iowa 1	1.67	2.27	0.23	0.31	0.54	0.64	70.6	0.49	0.67	0.15	0.19
6	Iowa 2[‡]	0.87	1.17	0.12	0.16	0.27	0.33	46.4	0.47	0.63	0.14	0.18
7	Michigan 1	1.78	2.29	0.24	0.31	0.52	0.58	6.8	1.66	2.13	0.51	0.61
8	Michigan 2	1.63	1.97	0.22	0.27	0.27	0.33	29.4	1.15	1.39	0.36	0.39
9	Minnesota 1	2.38	2.55	0.32	0.35	0.52	0.64	63.5	0.87	0.93	0.27	0.26
10	Minnesota 2	0.86	1.10	0.12	0.15	0.52	0.66	68.9	0.27	0.34	0.08	0.10
11	Minnesota 3	0.90	1.11	0.12	0.15	0.27	0.31	68.8	0.28	0.35	0.09	0.10
12	Nebraska 1	13.72	19.13	1.88	2.62	4.78	5.91	<0.1	13.72	19.13	4.25	5.43
13	Nebraska 2[‡]	10.44	14.66	1.43	2.01	3.26	4.19	0.2	10.42	14.63	3.23	4.15
14	Nebraska 3[‡]	9.75	13.83	1.33	1.89	3.01	3.92	<0.1	9.75	13.83	3.02	3.92
15	Nebraska 4	8.89	11.54	1.22	1.58	2.24	3.11	2.5	8.67	11.25	2.68	3.19
16	Nebraska 5	6.43	9.01	0.88	1.23	1.7	2.14	<0.1	6.43	9.01	1.99	2.56
17	Nebraska 6[‡]	4.05	5.33	0.55	0.73	1.36	1.6	<0.1	4.05	5.33	1.25	1.51
18	Nebraska 7	2.55	3.40	0.35	0.46	0.61	0.73	0	2.55	3.40	0.79	0.96
19	Nebraska 8[‡]	1.68	2.30	0.23	0.31	0.41	0.54	0.6	1.67	2.29	0.52	0.65
20	Nebraska 9	0.61	0.80	0.08	0.11	0.18	0.23	17.1	0.51	0.66	0.16	0.19
21	N. Dakota 1	5.48	7.50	0.75	1.03	1.34	1.74	5.8	5.16	7.07	1.60	2.00
22	N. Dakota 2	4.01	5.19	0.55	0.71	1.18	1.45	23.9	3.05	3.95	0.95	1.12
23	N. Dakota 3	3.75	5.12	0.51	0.7	1.25	1.47	0.4	3.74	5.10	1.16	1.45
24	N. Dakota 4	3.59	4.62	0.49	0.63	1.11	1.31	4.5	3.43	4.41	1.06	1.25
25	N. Dakota 5[‡]	1.52	1.89	0.21	0.26	0.36	0.41	45.9	0.82	1.02	0.25	0.29
26	N. Dakota 6	1.28	1.8	0.17	0.25	0.29	0.35	1.4	1.26	1.77	0.39	0.50
27	N. Dakota 7[‡]	0.74	0.95	0.1	0.13	0.23	0.27	12.0	0.65	0.84	0.20	0.24
28	S. Dakota 1	7.22	10.97	0.99	1.5	2.76	3.28	0.4	7.19	10.93	2.23	3.10

29	S. Dakota 2‡	4.25	6.07	0.58	0.83	1.99	2.57	<0.1	4.25	6.07	1.32	1.72
30	S. Dakota 3	1.97	2.77	0.27	0.38	0.79	0.95	30.0	1.38	1.94	0.43	0.55
31	S. Dakota 4‡	1.86	2.42	0.26	0.33	0.61	0.79	37.1	1.17	1.52	0.36	0.43
32	S. Dakota 5‡	0.93	1.22	0.13	0.17	0.38	0.52	16.9	0.77	1.01	0.24	0.29
33	Wisconsin 1	1.64	2.03	0.22	0.28	0.75	0.73	41.9	0.95	1.18	0.30	0.33
34	Wisconsin 2‡	1.20	1.58	0.16	0.22	0.48	0.54	49.8	0.60	0.79	0.19	0.23
35	Wisconsin 3‡	0.53	0.65	0.07	0.09	0.18	0.23	39.8	0.32	0.39	0.10	0.11
	Total	*112.2*	*152.3*‡‡	*15.3*	*20.8*	*35.3*	*43.8*		*99.7*	*136.4*	*30.9*	*38.7*

* N fertilizer application in kg N ha^{-1}
‡ Biomass collection area crosses state boundaries.
§ Biorefinery placements associated with biorefinery ID are presented in Figure S2.
†† Maximum currently grazed lands are estimated from 2008 CDL data.
‡‡ Total biomass production 261.7 Mg×10^6

Supplementary Table 4. EPIC modeled biomass and cellulosic ethanol production and calculated biofuel offset credits for three different collection radii without inclusion of grazing lands, assuming 90% harvest efficiency and fertilization level of 68 kg N ha^{-1}.

Collection Radius	Biomass production	Fossil fuel offset
km	*Mg×10^6*	*Mg CO_2e×10^6*
40	108.0	30.8
80	136.4	38.7
120	120.9	34.3

Supplementary Table 5. Comparison of state-wide biomass production estimated by EPIC's simulation of successional biomass on unfertilized marginal lands vs. the Billion Ton Study's[1] extrapolation of upland switchgrass to marginal and arable lands. The R^2 value is 0.0079 and the Spearman rank-order correlation coefficient (r_s) is -0.0061 with a two-tiled p-value of 0.98. An r_s value below 0 implies negative agreement between the two rankings.

	Average Biomass Production	
State	EPIC model	Billion Ton Study
	Mg ha^{-1}	
Illinois	8.16	12.50
Indiana	8.35	13.07
Iowa	7.81	11.73
Michigan	9.98	7.44
Minnesota	10.63	6.04
Nebraska	6.01	8.87
North Dakota	5.55	4.59
Ohio	7.16	14.03
South Dakota	4.75	7.59
Wisconsin	8.96	9.23
Area-weighted average	6.00	8.81

Supplementary Table 6. Estimates of CO_2-equivalent emissions from fuel used for field operations[†]; all fuel is assumed to be diesel with a carbon content of 85%.

Field Operation	Fuel Consumption	CO_2e Emission	Source
	L ha^{-1}	*g CO$_2$ m^{-2} yr^{-1}*	
Plowing [‡]			
Moldboard	21.8	5.6	*12*
Chisel	10.1	2.6	*13*
Soil finishing	7.4	1.7	*13*
Fertilizer application	9.8	2.6	*12*
Herbicide application	1.8	0.5	*13*
Cultivation	5.1	1.3	*13*
Rotary hoe	2.6	0.7	*13*
Planting	4.9	1.3	*12*
Harvest			
Baling (round)	7.4	1.9	*13*
Mowing [¶]	1.3	0.4	*14*
Forage raking	2.2	0.6	*13*
Alfalfa baling [¶]	1.2	0.3	*14*
Hay cut [*]	4.1	1.1	*15*
Haylage [*]	13.1	3.4	*15*
Soybean	11.1	2.9	*12*
Wheat [§]	11.1	2.9	*13*
Corn	11.5	3.0	*13*
Forage	17.4	4.5	*13*
Poplar	21.3	5.5	*16*

[†] All reported values were converted to L ha^{-1} if reported otherwise. The diesel energy content was assumed to be 36.4 MJ L^{-1} [17].

[‡] Moldboard plowing was conducted during 1989-1997, and chisel plowing during 1997-2009.

[¶] Fuel usage depends on crop yield; value given per yield of Mg ha^{-1}.

[*] Equipment used in calculation: for chopped forage (hay silage) a pull type pickup head 12 ft; for hay a rotary mower-conditioner 12 ft.

[§] Wheat and soybean harvest operations were assumed to consume equivalent amounts of energy.

Supplementary Table 7. Estimates of CO_2-equivalent (CO_2e) emissions associated with farming inputs other than fuel (see Supplementary Table 6).

Input	CO_2e emissions	Active ingredient	Source
	kg CO_2e kg^{-1}	*g L^{-1}*	
Fertilizer			
N	4.5		*18*
P	0.7		*13*
K	0.6		*12*; *13*
Lime	0.4		*12*
Herbicides †			
Accent	3.5	750	
Assure II	0.5	105	
Atrazine	2.3	479	
Basagran	2.3	479	
Bladex	4.2	900	
Broadstrike + Dual	4.3	925	
Buctril Gel	2.3	479	
Callisto	2.3	479	
Canopy	3.5	750	
Dimate 4E	2.3	479	
Dual II Magnum	3.9	824	
Dual Magnum	3.9	837	
Galaxy	2.3	490	
Goal	4.5	954	
Harmony Extra	0.0	10	
Lexar	1.9	404	
Lorox	2.4	500	
Marksman	1.8	393	
Princep	2.0	420	
Poast Plus	0.6	130	
Roundup	2.5	490	
Stinger	1.9	409	
Sevin 80	3.8	800	
Sencor	3.5	750	
First Rate	3.9	840	
Seeds			
Alfalfa	9.6		*12*
Wheat	0.4		*12*
Soybean	0.9		*12*
Corn	3.9		*12*
Red clover‡	6.3		*12*
Rye grass‡	2.0		*12*

† We assume emission of 4.7 kg CO_2 kg^{-1} herbicide active ingredient (*13*). Active ingredients concentrations were obtained as g L^{-1} or percent from the manufacturer's labels:

Accent – DuPont (2011) Accent herbicide material safety data sheet, du Pont Canada Company P.O. Box 2200, Streetsville, Mississauga, ON L5M 2H3, Canada. Available at www2.dupont.com/Crop_Protection/en_CA/assets/downloads/20110209%20Accent%20Herbicide%2013197.pdf. Accessed February 23, 2012.

Assure II – DuPont (2011) Assure II herbicide material safety data sheet, du Pont Canada Company P.O. Box 2200, Streetsville, Mississauga, ON L5M 2H3, Canada. Available at www2.dupont.com/Crop_Protection/en_CA/assets/downloads/20110309%20Assure%20II%20E%20MSDS.pdf. Accessed February 23, 2012.

Atrazine – SipcamAdvan (2010) Atrazine herbicide material safety data sheet, SipcamAdvan 2520 Meridian Parkway, Suite 525, Durham, NC 21173. Available at www.cdms.net/LDat/ld3QT008.pdf. Accessed February 23, 2012.

Basagran - BASF Canada Inc. (2009) Basargan herbicide material safety data sheet, BASF Canada Inc. 100 Milverton Drive Mississauga, ON L5R 4H1, Canada. Available at https://agro.basf.ca/West/Products/Product_Labels/BASAGRAN_Label_2011_West.pdf. Accessed February 23, 2012.

Bladex – AgNova Technologies (2008) Bladex herbicide material safety data sheet, AgNove Technologies, Doncaster Road, Doncaster East Vic 3109, Australia. Available at www.agnova.com.au/resources/Bladex-herbicide-msds.pdf. Accessed February 23, 2012.

Broadstrike + Dual – Dow AgroSciences (2009) Broadstrike + Dual herbicide material safety data sheet, Dow AgroSciences Canada Inc. Calgary, Alberta, Canada, T2P 5H1. Available at http://msdssearch.dow.com/PublishedLiteratureDAS/dh_02a3/0901b803802a3432.pdf?filepath=ca/pdfs/noreg/010-21022.pdf&fromPage=GetDoc. Accessed February 23, 2012.

Buctril – Bayer CropScience (2011) Buctril herbicide material safety data sheet, Bayer CropScience, Alexander Drive Research Triangle PK, NC 27709, USA. Available at http://fs1.agrian.com/pdfs/Buctril_Herbicide_%2829_Version_23_09102003%29_MSDS.pdf. Accessed February 23, 2012.

Callisto – Syngenta (2010) Callisto herbicide material safety data sheet, Syngenta Crop Protection Inc. P.O. Box 18300, Greensboro, NC 27419 USA. Available at www.syngentacropprotection.com/pdf/msds/03_994007162010.pdf. Accessed February 23, 2012.

Canopy – DuPont (2011) Canopy herbicide material safety data sheet, du Pont Canada Company P.O. Box 2200, Streetsville, Mississauga, ON L5M 2H3, Canada. Available at http://msds.dupont.com/msds/pdfs/EN/PEN_09004a35805aa981.pdf. Accessed February 23, 2012.

Dimate 4E – Winfield Solutions (2008) Dimate 4E herbicide material safety data sheet, Winfield Solutions, P.O. Box 64589, St. Paul, MN 55164, USA. Available at http://www.cdms.net/LDat/mp44N000.pdf. Accessed February 23, 2012.

Dual II Magnum – Syngenta (2010) Dual II Magnum herbicide material safety data sheet, Syngenta Crop Protection Inc. P.O. Box 18300, Greensboro, NC 27419 USA. Available at www.syngentacropprotection.com/pdf/labels/SCP818AL1N0809n.pdf. Accessed February 23, 2012.

Dual Magnum – Syngenta (2010) Dual Magnum herbicide material safety data sheet, Syngenta Crop Protection Inc. P.O. Box 18300, Greensboro, NC 27419 USA. Available at www.syngentacropprotection.com/pdf/labels/SCP816AL1U1210.pdf. Accessed February 23, 2012.

Galaxy – DuPont (2010) Galaxy herbicide material safety data sheet, du Pont Canada Company P.O. Box 2200, Streetsville, Mississauga, ON L5M 2H3, Canada. Available at www2.dupont.com/Crop_Protection/en_CA/assets/downloads/20090408%20-%20Galaxy%20E%20MSDS%20Cover%20Sheet.pdf. Accessed February 23, 2012.

Goal – Dow AgroSciences (2007) Goal herbicide material safety data sheet, Dow AgroSciences Canada Inc. Calgary, Alberta, Canada, T2P 5H1. Available at http://msdssearch.dow.com/PublishedLiteratureDAS/dh_005c/0901b8038005ccf2.pdf?filepath=au/pdfs/noreg/012-10170.pdf&fromPage=GetDoc. Accessed February 23, 2012.

Harmony Extra – DuPont (2008) Galaxy herbicide material safety data sheet, du Pont Canada Company P.O. Box 2200, Streetsville, Mississauga, ON L5M 2H3, Canada. Available at http://msds.dupont.com/msds/pdfs/EN/PEN_09004a35803ee645.pdf. Accessed February 23, 2012.

Lexar – Syngenta (2011) Lexar herbicide material safety data sheet, Syngenta Crop Protection Inc. P.O. Box 18300, Greensboro, NC 27419 USA. Available at www.syngentacropprotection.com/pdf/labels/SCP1201AL1D0209nn.pdf. Accessed February 23, 2012.

Lorox – DuPont (1984) Lorox herbicide material safety data sheet, du Pont Canada Company P.O. Box 2200, Streetsville, Mississauga, ON L5M 2H3, Canada. Available at www.cdms.net/ldat/mp9D5004.pdf and http://pmep.cce.cornell.edu/profiles/herb-growthreg/fatty-alcohol-monuron/linuron/herb-prof-linuron.html. Accessed February 23, 2012.

Marksman – BASF Canada Inc. (1986) Marksman herbicide material safety data sheet, BASF Canada Inc. 100 Milverton Drive Mississauga, ON L5R 4H1, Canada. Available at www.clearfield.ca/basf/agprocan/agsolutions/WebASProduct.nsf/WebDocCodeEast/Marksman/$File/Marksman.pdf. Accessed February 23, 2012.

Princep – Syngenta (2011) Princep herbicide material safety data sheet, Syngenta Crop Protection Inc. P.O. Box 18300, Greensboro, NC 27419 USA. Available at www.syngentaprofessionalproducts.com/pdf/labels/SCP526AL57K0608.pdf. Accessed February 23, 2012.

Poast Plus – BASF (2009) Poast Plus herbicide material safety data sheet, BASF 26 Davis Drive Research Triangle Park, NC 27709, USA. Available at www.cdms.net/LDat/ld00H006.pdf. Accessed February 23, 2012.

Roundup – DuPont (2011) Roundup herbicide material safety data sheet, du Pont Canada Company P.O. Box 2200, Streetsville, Mississauga, ON L5M 2H3, Canada. Available at www2.dupont.com/Crop_Protection/en_CA/assets/downloads/20110112%20Roundup%20WeatherMax%20Eng%20MSDS.pdf. Accessed February 23, 2012.

Stinger – Dow AgroSciences (2009) Stinger herbicide material safety data sheet, Dow AgroSciences Canada Inc. Calgary, Alberta, Canada, T2P 5H1. Available at www.cdms.net/LDat/ld02P044.pdf. Accessed February 23, 2012.

Sevin 80 – Bayer Environmental Science (2011) Sevin 80 herbicide material safety data sheet, Bayer Environmental Science, 95 Chestnut Ridge Road, Montvale, NJ 07645, USA. Available at www.cdms.net/LDat/mp5FD006.pdf. Accessed February 23, 2012.

Sencor – Bayer CropScience (2011) Sencor herbicide material safety data sheet, Bayer CropScience, 160 Quarry Park Blvd, SE Calgary, Alberta, T2C 3G3, Canada . Available at www.bayercropscience.ca/English/LabelMSDS/425/File.ashx. Accessed February 23, 2012.

First Rate– Dow AgroSciences (2003) First Rate herbicide material safety data sheet, Dow AgroSciences 9330 Zionsville Road, Indianapolis, IN, 46268 USA. Available at www.cdms.net/ldat/mp24M001.pdf. Accessed February 23, 2012.

‡ Cover crops

Supplementary Table 8. Estimates of total CO_2e emissions associated with farming of individual crops in areal (g CO_2e m^{-2} yr^{-1}) and energy intensity (g CO_2e MJ^{-1}) units. Emissions per areal unit are based on Supplementary Tables 6 and 7. Emissions per unit of energy for annual crops are calculated from GREET Version 1.8d.1, except for soybean. Soybean and perennial systems energy intensities are calculated from measured values at KBS. Average rotational values of CO_2e emissions (g CO_2e m^{-2} yr^{-1}) for the corn-soybean-wheat rotation appear in Table 1 of the main text.

Tillage	Corn	Soybean	Wheat	Poplar	Alfalfa	Suc*	Suc+N*
			g CO_2e m^{-2} yr^{-1}				
Conventional	73.0	10.2	41.5	-	-	-	-
No-till	72.9	11.1	40.3	7.1	39.9	4.4	63.1
			g CO_2e MJ^{-1}				
Conventional	37.7	7.1	37.8	-	-	-	-
No-till	34.7	6.8	35.6	2.3	8.0	1.0	9.9

* CO_2e emissions include harvest, feedstock transportation, and (for Successional + N) N fertilizer application.

Supplementary Table 9. Greenhouse gas (GHG) fluxes in the studied ecosystems (1989 – 2010, except as noted)[*]. Results shown are mean (± standard error), n = 4 replicate blocks. Statistically significant differences (ANOVA repeated measurements, $p < 0.05$) within columns are indicated by different letters.

System	N_2O-N	CH_4-C
	g $ha^{-1}d^{-1}$	
Conventional tillage C-S-W [†]	2.0 (0.3) [a]	-0.7 (0.1) [a]
No-till C-S-W	2.0 (0.2) [a]	-0.7 (0.1) [a]
Alfalfa	1.9 (0.2) [a]	-0.8 (0.0) [b]
Poplar	1.0 (0.2) [b]	-0.6 (0.0) [a,b]
Successional	0.6 (0.0) [c]	-0.9 (0.1) [b]
Successional + N [‡]	1.6 (0.3) [a]	-1.0 (0.4) [a,b]

[*] Average fluxes are calculated from fluxes measured when soils are unfrozen (March to November/December). We assume negligible fluxes during January – February when soils are mostly frozen: (1) fluxes measured in March immediately after soil thaw are the same or significantly lower than average March-December fluxes except for the Successional site; March fluxes were: Conventional tillage 1.0±0.2 (n=8 dates); No-till 1.3±0.2 (n=8); Alfalfa 2.0±0.8 (n=7); Poplar 0.7±0.2 (n=13); and Successional 1.3±0.1 (n=8) g N_2O-N ha^{-1} d^{-1}. Likewise, average pre-frost fluxes in November/December were similar (2 sites) or lower (5 sites) than the March-December average: Conventional tillage 0.7±0.1; No-till 0.8±0.1; Alfalfa 1.1±0.2; Poplar 0.5±0.2; and Successional 0.5±0.1 g N_2O-N ha^{-1} d^{-1} (n=16 dates for all sites). (2) Average soil concentrations of NO_3^--N to 25 cm during March and December were low relative to peak concentrations during the growing season (July) in all systems but the Successional: Conventional tillage N concentrations were 1.2±0.1, 1.8±0.1, and 9.9±0.7 μg NO_3^--N g^{-1} soil for December, March, and July, respectively; corresponding values for No-Till were 0.9±0.1, 1.4±0.1, and 8.0±0.7; for Poplar 0.3±0.1, 0.5±0.1, and 2.1±0.3; for Alfalfa 3.2±0.2, 2.3±0.1, and 5.6±0.2; for Successional 0.4±0.1, 0.6±0.1, and 0.5±0.1.

[†] Corn-Soybean-Wheat rotation

[‡] GHG fluxes from fertilized Successional system plots were measured in fertilized micro-plots within the Successional plots between the years 2008 – 2010.

Supplementary Table 10. Annual soil carbon change in A/Ap horizon and GHG impact (Supplementary Equation 2) over the period 1989 – 2001. There were no significant soil carbon changes in deeper horizons to 1m. Results are shown as mean difference from the conventional system, ±s.e., n = 6. From (*7*).

System	Soil carbon †	GHG impact
	kg C m^{-2}	*g CO_2e m^{-2} yr^{-1}*
Conventional tillage C-S-W	0.0 (0.1)[a,‡]	0.0 (30.6)
No-till C-S-W	0.4 (0.1)[b]	-122.2 (30.6)
Alfalfa	0.4 (0.3) [a,b]	-122.2 (91.7)
Poplar	-0.2 (0.5) [a,b]	61.1 (152.8)
Successional¶	1.3 (0.1) [c]	-397.2 (30.6)

† Positive values mean soil carbon gain and negative values carbon loss.
‡ Statistically significant differences in SOC concentration (ANOVA repeated measurements, $p < 0.05$) are indicated by different letters within column.
¶ Successional and Successional + N ecosystems assumed to be equal.

Supplementary Table 11. Fossil fuels offset credits.

System	Corn grain	Wheat grain	Soybean grain	Wheat straw	Alfalfa	Poplar	Suc	Suc + N
				g CO_2e MJ^{-1}				
Conventional C-S-W	25.9	21.4	225.6	108.3	-	-		-
No-till C-S-W	28.9	23.2	225.9	108.3	-	-		-
Cellulosic feedstock	-	-	-	-	103.3	105.0	107.3	98.4

Supplementary Table 12. Distribution of different slopes (%) across Land Capability Classes (LCC) IV – VII in the US Midwest as a percentage of the total acreage in each LCC. Because sloped marginal lands (LCC V-VII) are of a similar extent (20.1%) to cropped arable lands in LCC IV (20.9%), slope per se should pose little impediment to potential use for perennial cellulosic crops.

Slope	Land Capability Class			
	IV	V	VI	VII
%	% of LCC Area			
0 – 10	79.2	99.9	81.8	71.6
11 - 15	14.0	0.1	10.4	16.1
16 - 19	6.9	0.0	7.8	12.3

Supplementary Equations

Supplementary Eq 1: Ethanol production from marginal lands in regional simulations by EPIC

We used the following equation to convert biomass yields into liters of ethanol:

Ethanol production = Biomass Yield × 0.06 km × 0.06 km × 380.0 L Mg^{-1} × 100 (Eq 1)

= Biomass Yield × 136.8

where Biomass Yield (Mg ha^{-1}) is biomass production, 0.06 × 0.06 km is the cell size of the model, 380.0 L Mg^{-1} is the conversion factor for converting cellulosic biomass to ethanol[2], and 100 is number of hectares in 1 km^2.

Supplementary Eq 2: Soil Carbon CO_2e calculation

CO_2e for soil C change was calculated from carbon in soil cores collected in 2001 (Supplementary Table 10 and [7]):

$$CO_2e(SOC)\ g\ CO_2 \times m^{-2}\ yr^{-1} = \frac{(x_1 - x_2)\ kg\ C}{m^2 \times x_3\ yr} \times \frac{44\ kg\ CO_2}{12\ kg\ C} \times \frac{10^3\ g\ CO_2}{1\ kg\ CO_2} \quad \text{(Eq 2)}$$

where x_1 is soil C in the target system (in kg C m^{-2}), x_2 is soil C in the original reference system (Conventional tillage), and x_3 is the period of C accumulation (yr since transition; or 12 yr).

Supplemental Eq 3 and 4: N_2O and CH_4 CO_2-equivalents calculation

The CO_2-equivalents (g CO_2e m^{-2} yr^{-1}) for N_2O and CH_4 emissions were calculated using the IPCC 100-year horizon factors (298 for N_2O and 25 for CH_4)[19]:

$$CO_2e(N_2O) = \frac{x_1\ g\ N_2O - N}{ha \times d} \times \frac{44\ g\ N_2O}{28\ g\ N_2O - N} \times \frac{365\ d}{1\ yr} \times \frac{1\ ha}{10^4\ m^2} \times \frac{298\ g\ CO_2}{1\ g\ N_2O} \quad \text{(Eq 3)}$$

$$CO_2e(CH_4) = \frac{x_2\ g\ CH_4 - C}{ha \times d} \times \frac{16\ g\ CH_4}{12\ g\ CH_4 - C} \times \frac{365\ d}{1\ yr} \times \frac{1\ ha}{10^4\ m^2} \times \frac{25\ g\ CO_2}{1\ g\ CH_4} \quad \text{(Eq 4)}$$

where x_1 is the average daily N_2O-N emission rate (g N ha^{-1} d^{-1}) and x_2 is the average daily CH_4-C emission rate (g C ha^{-1} d^{-1}). Average fluxes of N_2O and CH_4 for all studied systems are given in Supplementary Table 1. Measurements of soil GHG fluxes were performed bi-weekly using a static-chamber method; for details see[18]. Cumulative emissions of N_2O (g N_2O – N ha^{-1}) and CH_4 (g CH_4 – C ha^{-1} d^{-1}) for each plot were determined by interpolating daily fluxes between sampling days over the course of the entire growing season from first thaw until the onset of frozen soils during 1989 - 2010. Average daily flux (g N_2O – N or CH_4 – C ha^{-1} day^{-1}) for each plot was

calculated by dividing the cumulative emissions for that plot by number of days in the year (365), assuming negligible fluxes to occur during winter when soils remain mostly frozen, but see Table S9 for details on fluxes during the soil thawing period. Average daily fluxes in row crop rotations were determined from rotational averages. For this we calculated cumulative emissions for each crop year as above and divided cumulative emissions by number of days in a given crop year.

Supplementary Eq 5: Farming CO_2 emissions equivalents

We assume 100% oxidation of diesel fuel (represented by the formula $C_{16}H_{34}$) to CO_2[18]:

$$CO_2e(\text{diesel}) = \frac{x_1\,L\,C_{16}H_{34}}{ha \times yr} \times \frac{832\,g\,C_{16}H_{34}}{1\,L\,C_{16}H_{34}} \times \frac{192\,g\,C}{226\,g\,C_{16}H_{34}} \times \frac{44\,g\,CO_2}{12\,g\,C} \times \frac{1\,ha}{10^4\,m^2} \qquad \text{(Eq 5)}$$

where x_1 is average annual diesel use for the field operation (L ha^{-1} yr^{-1}).

Supplementary Eq 6: Energy Equivalent calculation

$$\text{Energy Equivalent}(MJ\,ha^{-1}\,yr^{-1}) = DM \times X\frac{kg\,Fuel}{kg\,DM} \times Y\frac{L\,Fuel}{kg\,Fuel} \times \text{Biofuel}_{\text{energy}} \qquad \text{(Eq 6)}$$

where DM is dry mass of biomass yield (kg ha^{-1} yr^{-1}; Supplementary Table 2), X is the conversion factor for biofuel production from grain, straw, stover, or cellulosic feedstocks, Y is a factor accounting for fuel specific density, and $\text{Biofuel}_{\text{energy}}$ is biofuel energy content (MJ L^{-1}).

Supplementary Eq 7-8: GHG emission intensity of biofuel energy production

The GHG emission intensity (g CO_2e MJ^{-1}), defined here as the net CO_2e balance per unit of biofuel energy produced in the system:

$$\text{GHG emission intensity} = \frac{\text{Net } CO_2e \text{ balance}}{\text{Biofuel energy content}} \qquad \text{(Eq 7)}$$

where Biofuel energy content is the net biofuel energy yield of the system in MJ m^{-2} yr^{-1} and Net CO_2e balance (g CO_2e m^{-2} yr^{-1}) is:

$$\text{Net } CO_2e \text{ balance} = \sum CO_2e(\text{GHG}, \text{FF}, \text{Farm}, \text{Soil C}) \qquad \text{(Eq 8)}$$

where GHG is field fluxes of N_2O and CH_4, FF is fossil fuel offset credit, Farm is emissions associated with farming practices, and Soil C is changes in soil C concentrations under different tillage practices, all in g CO_2e m^{-2} yr^{-1}.

Supplementary Methods

Site-specific EPIC simulations

We used site-scale simulations based on specific data to calibrate the EPIC model before applying it to the regional-scale simulations. For calibration purposes, we used data from two Long-term Ecological Research (LTER) sites, KBS in Michigan (kbs.lternet.edu) and Cedar Creek (CDR) in Minnesota (cdr.lternet.edu), to model aboveground net primary productivity (NPP) of successional vegetation growing on former agricultural fields.

For EPIC simulations of aboveground net primary productivity (ANPP) of successional fields at KBS we used historical weather, terrain characteristics, and soil properties of the site. The Successional treatment at KBS was initiated in 1989 when agricultural management ceased and natural vegetation was allowed to re-establish. Spring burning began in 1997 to inhibit colonization of woody species. Dominant species include *Solidago canadensis*, *Elytrigia repens*, *Poa pratensis*, *Aster pilosus*, *Phleum pratense*, *Trifolium pratense*, *Apocynum cannabinum*, *Daucus carota*, *Hieracium spp.*, and *Rhus typhina* (http://lter.kbs.msu.edu/).

For EPIC calibration with KBS LTER results, we simulated composition of the successional plant community with three species previously parameterized for EPIC (*Poa pratensis*, *Phleum pratense*, and *Trifolium pratense*) with information on radiation use efficiency, leaf area index, stomatal conductance, and other physiological attributes. Colonization of competing woody species was simulated with a stand of poplar (*Populus* spp.) from 1989 until spring 1998 when it was terminated[20]. Spring burning (3 – 15 April) with 80% efficiency was simulated for the years 1997, 2003, 2004, 2006, and 2008. We simulated ANPP under three different scenarios, one without harvest and N fertilization, and two scenarios with fall harvest, one without N fertilization and one with N fertilization rates of 12.3 g N m^{-2} yr^{-1}. The scenario without fertilization and harvest included woody invasion and spring burning, while scenarios with fall harvest did not. For all scenarios, the EPIC model runs were based on historical records of daily maximum and minimum air temperature and precipitation from the KBS LTER dataset (http://lter.kbs.msu.edu/datatables). Daily solar radiation, relative humidity, wind speed, and missing temperature and precipitation were acquired from Gull Lake NWS weather station (42º 24’ N 85º 23’ W) also at KBS. Soil layer properties used in the simulations were those of the Kalamazoo soil series (fine-loamy, mixed, mesic Typic Hapludalf)[21].

ANPP simulated during EPIC calibration between years 2000 and 2008 averaged 600±110 g m^{-2} yr^{-1} for the scenario without biomass harvest and fertilization, which is similar to the observed average of 598±44 g m^{-2} (Table S2). Similarly, simulated ANPP for the scenario with harvest and fertilization was very close to field-based estimation, 960±80 vs. 879±64 g m^{-2} yr^{-1}.

Further, we validated EPIC model results for ANPP simulations with published field data from CDR. We used simulated weather, terrain characteristics, and soil layer properties to simulate ANPP of a 60-yr chronosequence experiment[22]. The 60-yr chronosequence at CDR was simulated according to the description in[22]. The chronosequence consisted of a series of 14 agricultural fields on Alfic and Typic Udipsamments[21] left unmanaged during periods ranging from one to 60 years. Floristic surveys conducted in 1987 revealed the presence of *Ambrosia artemisiifolia, Andropogon gerardii, Agropyron repens, Agrostris scabra, Polygonum convolvulus, Poa pratensis, and Schizachyrium scoparium*, among others. C_3 species appeared to dominate over C_4 species during the first half of the chronosequence period while an equal mix appeared to prevail during the second. The species composition during secondary succession appears to be consistent with that reported[23]. Due to lack of plant parameters for several species and uncertainty in their temporal occurrence and dominance, we used an equal mix of generic C_3 and C_4 plant parameterizations and simulated daily weather generated from data of the weather station at Rosemount, MN, near CDR. Weather parameters were used to simulate ANPP during a 60-yr period intended to approximate environmental conditions for 1928 – 1987. The only simulated external N addition was 7.7 kg ha^{-1} via wet deposition.

Direct comparisons of biomass productivity results are not possible for the CDR data because the simulations are not time specific. Simulated standing aboveground biomass during the July-August period averaged 513±113 g m^{-2} during the first three years. In comparison, (*22*) observed 509 g m^{-2} in the 1-yr old field and 296 g m^{-2} in the 3-yr old field. Simulated biomass during the last three years of the simulation averaged 767±127 g m^{-2}, while (*22*) observed 783 g m^{-2} in the 60-yr old field. While EPIC failed to capture the decrease in plant productivity observed during the first years of the chronosequence, it did capture the increase in productivity toward the end of the period. Similar to observations, simulated annual biomass productivity correlated moderately well with N mineralization and soil N. However, correlations obtained with observed data (R^2 = 0.78 for potential N mineralization; R^2 = 0.94 for soil N) (*24*) were considerably stronger than those obtained with simulated data (R^2 = 0.34 for net N mineralization; R^2 = 0.32 for soil N).

Overall, EPIC appeared to capture adequately the observed plant productivity patterns from both KBS and CDR LTER sites under different environmental constraints and management scenarios. In addition, (*24*) used EPIC for simulations of the effects of unmanaged grasses on soil carbon accrual on marginal lands in Nebraska, Kansas, and Texas and found good agreement between EPIC predictions and long-term field data, which provides further justification for using the model for large scale simulations.

KBS LTER vs. Regional Yields 1989-2009

Are KBS yields typical for the region? Yields (Mg ha^{-1} at standard moisture of 15.5% for corn and 13% for soybean and wheat) for KBS wheat and soybeans over our 21-year study period were similar to Kalamazoo County yields, which were similar to (soybean) or higher than (wheat) US national average yields (for soybean: 2.6±0.2 for KBS no-till vs. 2.5±0.1 for Kalamazoo County vs. 2.6±0.1 for the entire US; for wheat: 3.7±0.3 for KBS no-till vs. 3.4±0.1 for Kalamazoo County vs. 2.8±0.1 Mg ha^{-1} for the US from 1989-2009)[25].

KBS corn yields were more variable than County or national averages, likely reflecting the greater sensitivity of corn yield to midsummer periods of low rainfall and heat waves[26]. Overall average yields for KBS no-till corn (6.4±0.7 Mg ha^{-1}) were lower than county (7.4±0.2 Mg ha^{-1}) and national (8.4±0.2 Mg ha^{-1}) yields for 1989-2009. KBS corn yields were at or above county and national yields for 4 of the study's 9 corn years and not significantly different from, though lower than county and national yields, in 3 years. In 2 of the 9 corn years KBS yields were significantly lower than county and national averages. However, county and national data include yield from both irrigated and rainfed acreage, and thus would be expected to be higher than rainfed (non-irrigated) KBS yields. About 38% of Kalamazoo County and 15% of total US corn acreage is irrigated[27]. The well-drained loam soils at KBS make corn yields particularly sensitive to interannual variation in precipitation. For example, in 2008 (a drought year at KBS) rainfed yields at KBS were only ~60% of irrigated yields (7.5±0.3 vs. 12.3±0.2 Mg ha^{-1} for rainfed vs. irrigated corn, respectively). In contrast in 2011, a year with high summer precipitation at KBS, rainfed yields at KBS nearly matched irrigated yields (12.3±0.2 Mg ha^{-1} rainfed vs. 13.8±0.1 Mg ha^{-1} irrigated), and were well above the average from Kalamazoo County (10.2 Mg ha^{-1}). These data suggest that KBS corn yields are not atypical of those experienced by Kalamazoo County farmers, and reflect how yields from rainfed corn will vary given the year-to-year variability in local precipitation that is typical for the region.

Supplementary References

1. Perlack, R.D. & Stokes, B.J. (Leads) (2011) US Billion-Ton Update: Biomass Supply for a Bioenergy and Bioproducts Industry. Report to US Department of Energy. Oak Ridge National Laboratory, Oak Ridge, TN., p 227
2. Schmer, M.R., Vogel, K.P., Mitchell, R.B. & Perrin R.K. Net energy of cellulosic ethanol from switchgrass. *Proc. Natl. Acad. Sci. USA* **105**, 464-469. (2008).
3. Causarano, H.J. et al., Simulating field-scale soil organic carbon dynamics using EPIC. *Soil Sci. Soc. Am. J.* **71**, 1174-1185. (2007).
4. Wang, X., He, X., Williams, J.R., Izaurralde, R.C. & Atwood, J.D. Sensitivity and uncertainty analyses of crop yields and soil organic carbon simulated with EPIC. *Trans. ASABE* **48**, 1041-1054. (2005)
5. National Research Council, *Liquid Transportation Fuels from Coal and Biomass* (National Academies Press, Washington, D.C. 2009).
6. Gregg, J.S. & Izaurralde, R.C. Effect of crop residue harvest on long-term crop yield, soil erosion, and carbon balance: tradeoffs for a sustainable bioenergy feedstock. *Biofuels* **1**, 69 (2010)
7. Syswerda, S.P., Corbin, A.T., Mokma, D.L., Kravchenko, A.N. & Robertson, G.P. (2011). Agricultural management and soil carbon storage in surface vs. deep layers. *Soil Sci. Soc. Amer. J.* **75**, 92 (2011).
8. Gelfand, I. *et al.* Carbon debt of Conservation Reserve Program (CRP) grasslands converted to bioenergy production. *Proc. Natl. Acad. Sci. USA* **108**, 13864-13869 (2011)
9. Perlack, R.D. *et al.* Biomass as feedstock for a bioenergy and bioproducts industry: The technical feasibility of a billion-ton annual supply (2005) Available at: http://feedstockreview.ornl.gov/pdf/billion_ton_vision.pdf. Accessed August 26, 2011.
10. Heaton, E.A., Dohleman, F.G. & Long, S.P. Meeting US biofuel goals with less land: the potential of Miscanthus. *Global Change Biol.* **14**, 2000 (2008).
11. Monti A., Fazio S. & Venturi G. The discrepancy between plot and field yields: Harvest and storage losses of switchgrass. *Biomass Bioenerg.* **33**, 841 (2009).
12. West, T.O. & Marland, G. A synthesis of carbon sequestration, carbon emissions, and net carbon flux in agriculture: comparing tillage practices in the United States. *Agr. Ecosys. Environ.* **91**, 217 (2002).
13. Lal, R. Carbon emission from farm operations. *Environ. Int.* **30**, 981 (2004).
14. Adler, P.R., Del Grosso, S.J. & Parton, W.J. Life-cycle assessment of net greenhouse-gas flux for bioenergy cropping systems. *Ecol. App.* **17**, 675,(2007).
15. Stein, D. "2008-2009 Custom Machine and Work Rate Estimates. District Farm Business Management" (Michigan State University Extension, East Lansing, Michigan, 2009). http://www.msu.edu/user/steind/

16. Luger, E. *Tech. Report No. B10157* (European Energy Crops *Inter*Network, 1998).
17. Oak Ridge National Laboratory (ORNL), (2003). Available at: http://www.localenergy.org/pdfs/Document%20Library/Bioenergy%20conversion%20factors.pdf. Accessed August 26, 2011.
18. Robertson, G.P., Paul, E.A., Harwood, R.R. Greenhouse gases in intensive agriculture: Contributions of individual gases to the radiative forcing of the atmosphere. *Science* **289**, 1922-1925 (2000)
19. Forster, P. *et al.*, in *Climate Change 2007: The Physical Science Basis. Contribution of Working Group I to the Fourth Assessment Report of the Intergovernmental Panel on Climate Change,* S. Solomon *et al.*, Eds. (Cambridge University Press, Cambridge, United Kingdom and New York, NY, USA, 2007), pp. 129-234.
20. Foster, B.L. & Gross, K.L. Temporal and spatial variability of woody plant establishment in Michigan old-fields. *Am. Midl. Nat.* **142**, 229 (1999).
21. Soil Survey Staff, Natural Resources Conservation Service, United States Department of Agriculture (USDA). Available at: http://soildatamart.nrcs.usda.gov. Accessed August 26, 2011.
22. Zak, D.R., Grigal, D.F., Gleeson, S. & Tilman, D. Carbon and nitrogen cycling during old-field succession: Constraints on plant and microbial biomass. *Biogeochemistry* **11**, 111 (1990).
23. Inouye, R.S. & Tilman, D. Convergence and divergence of old-field vegetation after 11 yr of nitrogen addition. *Ecology* **76**, 1872 (1995).
24. Izaurralde, R.C., Williams, J.R., McGill, W.B., Rosenberg, N.J. & Jakas, M.C.Q. Simulating soil C dynamics with EPIC: Model description and testing against long-term data. *Ecol. Model.* **192**, 362 (2006).
25. http://www.nass.usda.gov/Statistics_by_Subject/index.php (accessed October 4, 2012)
26. Hatfield, J. L. *et al.* Climate impacts on agriculture: implications for crop production. *Agronomy Journal* **103**, 351-370, doi:10.2134/agronj2010.0303 (2011).
27. http://quickstats.nass.usda.gov/ (accessed October 4, 2012)